Journal of Cardiovascular Magnetic Resonance 28 (2026) 102733

Contents lists available at ScienceDirect

Journal of Cardiovascular Magnetic Resonance

journal homepage: www.sciencedirect.com/journal/jocmr

Review Article

Clinical implications of vessel wall imaging—State-of-the-art review

Niranjan Balu[a], Gador Canton[a], Mahmud Mossa-Basha[a], Luca Saba[b], Scott McNally[c], Thomas Hatsukami[d], Chun Yuan[a,*]

[a] Department of Radiology, University of Washington, Seattle, Washington, USA
[b] Department of Medical Imaging, Azienda Ospedaliero Universitaria (A.O.U.) of Cagliari-Polo di Monserrato, Cagliari, Italy
[c] Department of Radiology, University of Utah, Salt Lake City, Utah, USA
[d] Department of Surgery, University of Washington, Seattle, Washington, USA

A B S T R A C T

Diseases of the arterial wall are best diagnosed using vessel wall magnetic resonance imaging (MRI) since luminal imaging does not show the extent of wall pathology. Intracranial and extracranial carotid artery pathology such as atherosclerosis, dissections, vasculitis, and occlusions can lead to clinically significant events such as stroke. Direct visualization of the arterial wall pathology using vessel wall MRI can direct clinical diagnosis and management. This review highlights the importance of carotid and intracranial vessel wall MRI and their clinical applications in neurovascular pathologies. Recent developments such as the carotid Plaque-Reporting and Data System risk scoring and intracranial vasculopathy differentiation using vessel wall MRI are reviewed. Technical requirements of vessel wall MRI sequences for clinical diagnosis and future diagnostic approaches such as stroke etiology reclassification are also discussed.

1. Introduction

Magnetic resonance (MR) vessel wall imaging (VWI) has dramatically improved vascular disease understanding, diagnosis, and in some instances patient care, over the past 30 years. MR VWI has been applied to all vascular beds throughout the body, but the most extensive investigation, evidence, and clinical applications have come from neurovascular MR VWI, specifically of the extracranial and intracranial vascular beds.

Early technical development of MR VWI was focused on carotid VWI because of the carotid plaque's role in causing stroke and the unique opportunity for histological validation using endarterectomy specimens as a reference standard. Comparing pre-surgical carotid VWI to histology enabled the identification of signal characteristics of plaque components: hyperintense signal (HIS) on T1-weighted magnetic resonance imaging (MRI) has been validated to correspond with the presence of intraplaque hemorrhage (IPH) [1,2]; lipid-rich necrotic core (LRNC) can be readily identified by its non-enhancement after gadolinium contrast administration [3–5]; hypointense signal on any MR weighting corresponds to calcification; fibrous cap integrity can be determined on VWI and it has been validated with histology [6,7]. The unique power of MRI for identifying IPH is of particular interest since IPH has been associated with an increased risk of stroke and transient ischemic attack (TIA) [8,9], as well as plaque growth [10]. Unlike conventional luminal (angiographic) imaging techniques that primarily focus on the degree of stenosis, VWI provides detailed characterization of the key plaque morphological and compositional features associated with the risk of future cerebrovascular events, establishing itself as an avenue for comprehensive plaque evaluation with a wide-ranging clinical potential. The advances in carotid VWI served as an impetus for the development of intracranial MR VWI techniques. Several clinical applications have spurred the rapid adoption of intracranial MR VWI in

Abbreviations: 3D-MERGE, 3D MSDE prepared rapid gradient echo; ASNR, American Society of Neuroradiology; BCVI, blunt cerebrovascular injury; CAIPI, controlled aliasing in parallel imaging; CTA, computed tomographic angiography; DANTE, delay alternating with nutation for tailored excitation; DSA, digital subtraction angiography; ESUS, embolic stroke of undetermined source; ICAD, intracranial atherosclerotic disease; IPH, intraplaque hemorrhage; LRNC, lipid-rich necrotic core; MATCH, multi-contrast atherosclerosis characterization; MPRAGE, magnetization prepared rapid gradient echo; MRI, magnetic resonance imaging; MSDE, motion-sensitized driven equilibrium; NASCET, North American symptomatic carotid endarterectomy trial; OR, odds ratio; PANCS, primary angiitis of the central nervous system; Plaque-RADS, plaque reporting and data system; RCVS, reversible cerebral vasoconstriction syndrome; SNAP, simultaneous non-contrast MRA and intraplaque hemorrhage imaging; SNR, signal-to-noise ratio; TIA, transient ischemic attack; TOAST, trial of org 10172 in acute stroke treatment; TOF, time-of-flight; vwE, vessel wall enhancement; VWI, vessel wall imaging

* Corresponding author.
E-mail address: cyuan@uw.edu (C. Yuan).

https://doi.org/10.1016/j.jocmr.2026.102733
Received 20 June 2025; Received in revised form 25 March 2026; Accepted 13 April 2026

the clinic and there is now an increasing interest in MR VWI applications [11,12].

There has been significant progress of MR VWI in recent years in terms of technical development, optimized applications in different vascular beds, specific analysis tools for quantitative vessel wall and atherosclerosis characterization, and potential clinical applications. Together, these developments further strengthen the translation of VWI to the clinic, mainly in extra and intracranial applications. While the scope of VWI applications is broad in terms of vascular beds and new research applications, clinical applications are expected to drive further adoption of VWI with carotid and intracranial applications accounting for the majority of immediate clinical VWI usage. Hence this state-of-the-art review will only focus on extracranial and intracranial MR-based VWI techniques and their clinical implications. Accordingly, VWI in the context of this manuscript denotes MR VWI unless specifically noted.

2. Clinical utilization of MR VWI

A survey of the American Society of Neuroradiology (ASNR) on the use of MR VWI in 2019 [12] showed that nearly 52% (214/411) of the 411 groups that responded were actively using MR VWI in their clinical practices, including 62% (134/217) of academic and 50% (83/166) of private practice respondents. Exactly 72% (154/214) of respondents indicated they were using MR VWI at least 1–2 times per month, with vasculopathy differentiation (94%, 201/213), cryptogenic stroke assessment (41%, 88/213), culprit intracranial atherosclerotic disease (ICAD) evaluation (40.5%, 84/213), and aneurysm assessment for rupture risk (38%, 81/213) being the most common uses. For those not using MR VWI, the primary reasons were a lack of clinician interest (56%, 110/194), limited interpretation expertise (53%, 103/194), knowledge of applications (50%, 98/194), lack of time or resources for protocol development (49%, 95/194), lack of technical support for protocol development (45%, 90/194), lack of standardized protocols (34%, 67/194), and long scan times (25%, 49/194). These primarily fall into a few categories: 1) limited education and understanding of technique value, clinical applications, and imaging interpretation, 2) lack of existing protocols or support for protocol development, and 3) long scan times limiting clinical implementation. Exactly 55% (124/220) of groups who were not using MR VWI indicated that if these obstacles were overcome, they would use the technique. Carotid vessel wall MR, which in the corresponding extracranial carotid survey [11], was used by 26% (107/411) of groups and most commonly for large-artery vasculitis assessment (63%), followed by plaque instability or IPH (61%, 55/90), and dissection detection/characterization (51%, 46/90). The lack of clinician interest (64%, 168/263) was the most common barrier to implementation followed by radiologist availability for protocol development (48%, 125/263) and limited knowledge of clinical applications (44%, 115/263) or interpretation expertise (45%, 118/263). These indicate the need for further education and awareness among clinicians of the current clinical applications made possible by MR VWI.

3. Vessel wall MRI scanning

3.1. Carotid VWI

Carotid vessel wall MRI was built on two-dimensional (2D) black-blood fast spin-echo imaging with the intent to cover the carotid bifurcation where most carotid plaques occur. Dedicated coils for carotid MRI were required to obtain adequate signal-to-noise ratio (SNR) at the carotid bifurcation [13,14]. With the use of carotid coils, 12 to 16 2-mm thick axial slices can be obtained with 0.6-mm in-plane resolution within a 3-to-5-minute scan time per contrast. Gadolinium contrast injection is recommended for LRNC visualization [3,4]. Plaque components can be identified based on their signal characteristics on different VWI contrasts. A typical 2D protocol consists of multiple contrasts (T1w, T2w, time-of-flight [TOF], proton density (PD) weighted, and post-gadolinium contrast T1w) for the identification and quantification of stenosis, fibrous cap status, IPH, LRNC, and plaque morphology [15]. Using this combination of contrasts, IPH can be identified as hyperintense region relative to adjacent muscle on T1-weighted contrasts (T1w and TOF) and by its non-enhancement on post-gadolinium T1w. LRNC can be identified primarily by its non-enhancement on post-gadolinium T1w. Calcification appears hyperintense on all VWI contrasts. Fibrous cap status can be identified as a band overlying LRNC on TOF and post-gadolinium T1w and the fibrous cap status (thin, thick, or ruptured) can be ascertained in relation to the lumen. With the increased availability of carotid coil configurations [16–19] and commercial versions becoming available, carotid vessel wall MRI is increasingly used clinically. Three-dimensional (3D) vessel wall MRI sequences have also been developed to overcome the limitations of 2D vessel wall MRI sequences such as low through-plane resolution and low SNR. 3D sequences with specialized newer black-blood imaging techniques [20–22] are also able to provide larger coverage, isotropic resolution, and good blood suppression with similar scan times as 2D sequences. A 0.63 to 0.7 mm isotropic sequence covering the entire extracranial carotids can be scanned within 2 min [23] to 6 min [24] depending on the sequence and resolution. A 0.7 mm isotropic resolution is sufficient for clinical evaluation of carotid plaque. Multiple contrast weightings (T1w, post-gadolinium T1w, TOF, highly T1-weighted, and T2w) are still recommended for complete plaque component quantification. If there is a need to reduce total scan time, then the number of sequences may be reduced based on the clinical diagnostic need. At a minimum, it is recommended to use T1w sequence with a post-gadolinium T1w sequence. A highly weighted T1w sequence should be added if IPH is of interest. T2w can be omitted if post-gadolinium T1w is available. While use of 3D sequences can allow carotid vessel wall MRI without the need for dedicated carotid coils [25], it is still recommended to use carotid coils when they are available to enable high SNR scans since this allows reducing scan times. According to a survey of the ASNR [11], the most frequently used extracranial VWI sequences pre-contrast T1-weighted (88.2% (75/85)) and postcontrast T1-weighted (83.5% (71/85)), T2-weighted (49.4% (42/85)), and 3D gradient recalled-echo (including magnetization prepared rapid gradient echo [MPRAGE]) (44.7% (38/85)). Consensus guidelines for both 2D or 3D protocols for carotid VWI are provided in [15]. Below, we briefly review the key technologies that underlie those protocols.

Plaque composition was initially characterized with a 2D carotid VWI multi-contrast protocol consisting of T1, T2, and PD weighted fast spin-echo sequences, combined with TOF sequence [26]. This protocol was further optimized to visualize the vessel wall by including blood suppression techniques that remove the blood flow signal within the lumen and fat suppression techniques to remove the signal from surrounding perivascular fat tissue. Double inversion recovery ([27]) for single slice 2D VWI and its modification for multi-slice application (multi-slice double inversion recovery [28]) can be used to acquire a stack of four to eight slices with good blood suppression. The signal features of different plaque components (IPH, LRNC, calcification and fibrous cap integrity, loose matrix) were identified from these optimized VWI protocols by comparison to histology [26].

Newer techniques have now enabled 3D carotid VWI protocols that provide a higher through-plane resolution and the possibility of isotropic voxel scans promoting clinical use of carotid VWI. The resulting 3D images can be reformatted into multiple orientations improving vessel wall and plaque visualization (Figs. 1 and 2). 3D fast spin-echo VWI sequences with variable flip angle trains [29] (termed SPACE [24] [Siemens], VISTA [30] [Philips], CUBE [31] [GE] or MATRIX [32] [United]) have some inherent blood suppression capability but dedicated blood suppression methods provide improved blood suppression. Motion-sensitized driven equilibrium (MSDE [21], also known

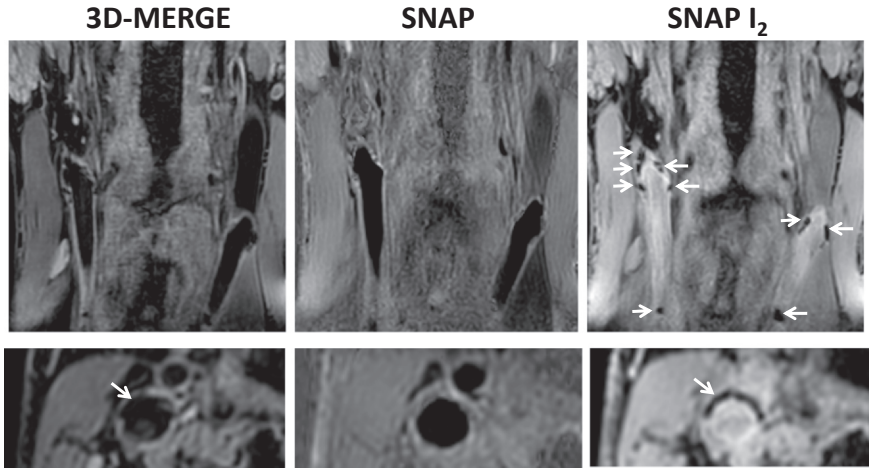

Fig. 1. Bilateral carotid plaques with several calcifications (arrows) can be seen using multi-contrast 3D VWI. The isotropic voxels of 3D VWI allow plaque visualization from multiple views. Coronal reformats are shown in the upper panel and axial reformats of the right carotid artery are shown in the lower panel. Multiple calcifications can be seen on the coronal reformat of the 3D-MERGE sequence (arrow of one calcification shown on the axial 3D-MERGE). Due to surface location of some calcifications, it may be difficult to differentiate them from the lumen on a black-blood sequence like 3D-MERGE (or SNAP—middle column). However, the SNAP I2 image (reference image of SNAP acquisition) has gray-blood contrast and allows easy identification of calcifications (arrows shown on SNAP I2). Axial reformat of SNAP I2 shows the semi-ring-shaped surface calcification clearly (arrow on axial SNAP I2). *3D* three-dimensional, *VWI* vessel wall imaging, *3D-MERGE* 3D MSDE prepared rapid gradient echo, *MSDE* motion-sensitized driven equilibrium, *SNAP* simultaneous non-contrast MRA and intraplaque hemorrhage imaging, *MRA* magnetic resonance angiography.

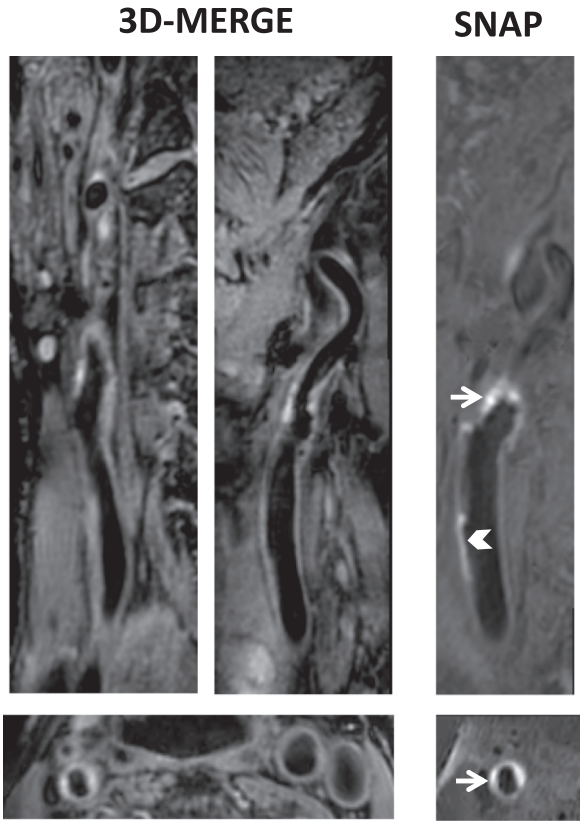

Fig. 2. Isotropic voxels of 3D-MERGE sequence allow reformatting in multiple planes allowing review of the atherosclerotic plaque at the right carotid bifurcation. The corresponding reformats of the right carotid on SNAP sequence show hyperintense signal (arrows) indicating intraplaque hemorrhage in this plaque. Note that there is also a proximal intraplaque hemorrhage in the right common carotid as indicated by hyperintense signal on SNAP (chevron). *3D* three-dimensional, *3D-MERGE* 3D MSDE prepared rapid gradient echo, *MSDE* motion-sensitized driven equilibrium, *SNAP* simultaneous non-contrast MRA and intraplaque hemorrhage imaging, *MRA* magnetic resonance angiography.

as flow-sensitized dephasing) and delay alternating with nutation for tailored excitation (DANTE [22]) are suited for blood suppression with 3D VWI and allow for fast 3D-MERGE [23] or DANTE prepared fast low-angle shot [33] sequences to assess plaque morphology. IPH can be assessed using 3D sequences without blood suppression methods such as MPRAGE [34] or using specialized reconstructions such as the SNAP (simultaneous non-contrast magnetic resonance angiography and intraplaque hemorrhage imaging) [35] sequence. Combination of multiple 3D weighted contrasts can be achieved, such as using the MATCH [36] sequence, but the combination sequence can have a longer scan time than each of the separate sequences it replaces. While the inherent registration of the image contrasts and reduction in total scan time using combination sequences are an advantage, it must be weighed against the potential for motion artifacts due to the longer scan time of the combination sequence.

Gadolinium contrast injection is recommended for the identification of LRNC. Initial studies in carotid VWI were based on T2w MRI [37]. Use of gadolinium was later shown to improve the identification of LRNC [3,38]. Hence, if gadolinium contrast injection is feasible, T2w contrast can be omitted. Pre- and post-contrast VWI using the same sequence parameters enable LRNC visualization by comparing the pre- and post-contrast signal since LRNC does not enhance after gadolinium injection and can be identified as a non-enhancing region. Specialized blood suppression methods (quadruple inversion recovery [39] for 2D VWI and MSDE [21] for 3D VWI) are needed to ensure the same blood suppression after contrast injection.

3.2. Intracranial VWI

Early publications on intracranial VWI used 2D turbo-spin echo techniques with thin slices (2 mm) and in-plane high-resolution (0.4 mm) to assess the vessel wall [40]. These techniques were easy to use on all MRI scanners but required focused imaging on specific arterial segments. This was due to the inability to perform large field-of-view scanning and the need to scan in multiple planes, which often resulted in long scan times. 2D scans required radiologist involvement to determine the appropriate scan plane but also limited lesion detection and assessment to stenotic lesions.

For these reasons, almost all institutions now rely on 3D acquisitions, which provide for high through-plane resolution, with thinner slices, and the ability to do multiplanar reconstructions with isotropic acquisitions (Fig. 3), facilitating shorter overall scans and global coverage. 3D protocols also reduce the reliance on real-time radiologist review during scan prescription since they can provide whole brain coverage. Most protocols use 3D variable refocusing flip angle sequences (known as VISTA/SPACE/CUBE/MATRIX on different scanner platforms). These techniques possess inherent blood suppression due to the flip angle sweep employed, making them a natural application for intracranial VWI. After gadolinium contrast administration, however, flow artifacts can present themselves due to gadolinium's shortening of

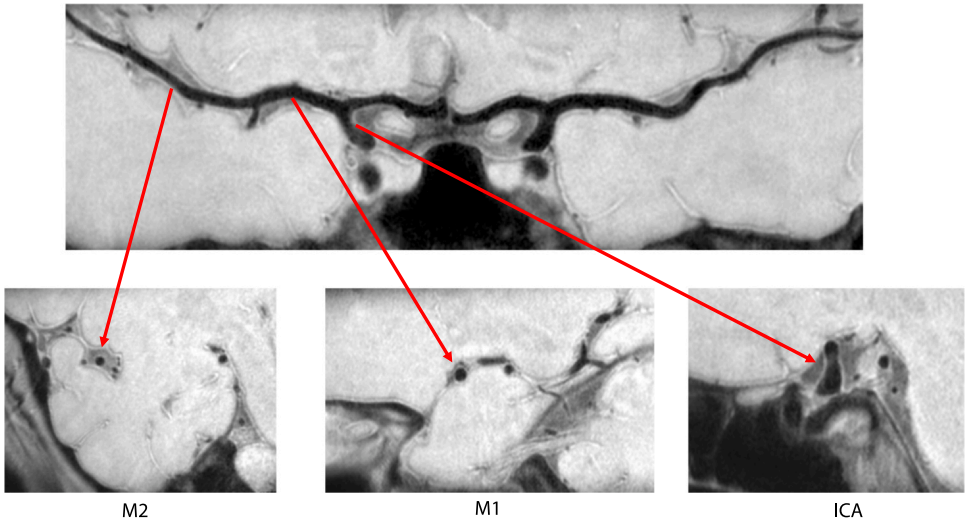

Fig. 3. High-resolution (0.4 mm isotropic) PD weighted DANTE VISTA of the intracranial arteries allows reformatting in multiple planes to view vessel wall structure. The upper panel shows curved planar reformat along the two middle cerebral arteries. The lower panel show reformats axial to the vessel at the levels indicated by red arrows. *PD* proton density, *DANTE* delay alternating with nutation for tailored excitation

the blood time-to-inversion. Flow suppression pre-pulses may be used to mitigate these flow artifacts, including MSDE [21] and DANTE [22]. DANTE blood-suppressed and controlled aliasing in parallel imaging (CAIPI)-accelerated 3D T1-weighted SPACE post-contrast intracranial VWI has shown significant improvement in qualitative evaluation of overall image quality, artifact, blood suppression, and motion artifact ratings when compared to conventional T1-weighted post-contrast SPACE intracranial VWI, however had significantly lower SNR [41]. DANTE blood-suppressed T1-weighted post-contrast SPACE showed significant improvement in qualitative image quality, SNR, blood suppression, artifact ratings, but without a significant difference in motion artifacts relative to conventional acquisition. Combining artificial intelligence (AI)-denoising algorithms with DANTE-CAIPI for post-contrast intracranial VWI showed equivalent SNR, but significantly improved image quality, blood suppression, and artifact ratings compared to conventional post-contrast intracranial VWI [42].

Scan times for intracranial VWI protocols can be challenging (longer than 7 min per sequence) considering the need for high resolution, in the range of 0.4 to 0.6 mm isotropic voxel size, combined with maintenance of SNR for adequate arterial wall visualization [43] and whole brain coverage. Advanced acceleration techniques can shorten scan times [44], while mitigating SNR drop [41]. Compressed sensing acceleration has also facilitated accelerated acquisition with equivalent SNR and image quality relative to reference scans [45,46]. Novel deep-learning denoising algorithms applied to intracranial VWI facilitate improved or equivalent image quality at a reduced scan time [42,47]. Similar to carotid VWI, if there is a need to minimize the number of contrasts acquired, then it is recommended to acquire a T1w sequence with a post-gadolinium T1w sequence at a minimum. Addition of a highly T1w weighted sequence can aid in the detection of IPH or thrombus [2,34,35,48]. According to a survey of the ASNR [12], the most frequently used intracranial VWI sequences are postcontrast T1-weighted (89.1% (188/211)), pre-contrast T1-weighted (88.6%, (187/211)), and T2-weighted (39.3%, 83/211).

4. Clinical utilization of vessel wall MRI

For carotid VWI, there has been more than 30 years of research [13] highlighting its value in assessing atherosclerotic plaque composition for stroke risk stratification [15]. While carotid atherosclerosis characterization is the main clinical use case for carotid VWI, it has also found clinical value in the diagnosis of carotid webs, dissections, and occlusions. Intracranial VWI, introduced in 1995 [49], reached broader usage after the first 3D publication in 2010 [30] and has been used for many clinical applications, including differentiation of intracranial vascular disease [50,51], aneurysm [52] and ICAD [53] characterization, prediction of aneurysmal subarachnoid hemorrhage complications [54], and determination of stroke etiology [55].

5. VWI in stroke evaluation

VWI is emerging as an important tool in stroke evaluation, particularly for understanding the underlying causes of ischemic stroke and guiding secondary prevention strategies. Since VWI provides a direct assessment of the arterial wall compared to traditional angiography, VWI is increasingly being adopted for detection of non-stenotic large-artery atherosclerosis. VWI also allows differentiation of vasculopathies recognized as probable causes of ischemic stroke, such as vasculitis and reversible cerebral vasoconstriction syndrome (RCVS) [50,51,56–58].

5.1. Carotid VWI features in stroke patients

Carotid atherosclerotic plaques are frequently found ipsilateral to a qualifying embolic stroke of undetermined source (ESUS) and often presenting with high-risk features [59–63]. In a single-center stroke registry study that included 1721 acute ischemic stroke patients [63], the etiology of up to 16% (88/545) of cases was reclassified after considering the presence of ipsilateral high-risk non-stenosing carotid plaque, with 22.6% (38/168) of cardioembolic cases being reclassified to multiple potential etiologies and 20.8% (41/197) of ESUS cases being reclassified to large-artery atherosclerosis. High-risk carotid plaques are also more often found in the ipsilateral than the contralateral carotid artery in patients with cerebral ischemic symptoms of known cause [64]. In fact, several studies that include cryptogenic (not necessarily ESUS) stroke patients have shown that non-stenosing carotid plaques with high-risk features are more prevalent ipsilateral to the infarct [65,66]. Non-stenosing ipsilateral high-risk carotid plaques were also more frequent in cryptogenic stroke patients compared to cardioembolic or small-vessel stroke patients [65,67]. The CAPIAS study showed that large-artery-stroke patients with 50–69% carotid stenosis presented the highest prevalence of ipsilateral high-risk plaques [65]. This finding, together with the reported high-risk plaque prevalence in arteries with $< 50\%$ stenosis ipsilateral to cryptogenic strokes [67], underscores the need to include VWI in the stroke workup to detect high-risk plaque features. Among the high-risk features, the most frequently reported feature of ipsilateral carotid plaque is IPH [62,65,66,68], regardless of stroke etiology. Larger LRNCs were also found ipsilateral to cryptogenic stroke patients compared to cardioembolic or small-vessel strokes. These VWI findings suggest that a subset of cryptogenic strokes may be caused by the non-stenosing

ipsilateral high-risk carotid atherosclerotic plaque, stressing the need to integrate carotid VWI clinically.

One of the limitations for VWI clinical integration has been variability in imaging protocols, interpretation, and reporting standards. The Carotid Plaque-RADS (Reporting and Data System) [69], recently introduced into clinical practice, represents a standardized method for assessing stroke risk by focusing not just on the degree of stenosis, but also on the characteristics of the carotid plaque itself. This scoring system acknowledges that patients with moderate stenosis, but high-risk plaque features, may have a stroke risk comparable to those with severe stenosis, while patients with severe stenosis but stable plaques may have a lower-than-expected risk and may not require immediate intervention.

The Plaque-RADS stratifies plaques into four main categories with intermediate subcategories to capture differences in plaque composition and vulnerability—a full documentation can be found in [69]. In addition to the primary categories, the Plaque-RADS system allows for the inclusion of "*ancillary features*" (such as inflammation, neovascularization, positive remodeling, plaque burden, progression of stenosis, and calcifications) and "*modifiers*" (e.g., limited diagnostic study, presence of a stent, or previous carotid endarterectomy). These supplemental descriptors enhance the reporting and risk stratification process, ensuring that each patient's imaging findings are communicated in a clear, standardized, and clinically actionable manner. Figs. 4 and 5 show examples of Plaque-RADS 3 and Plaque-RADS 4 category carotid plaques and their appearance on VWI.

Studies have demonstrated that incorporating Plaque-RADS scores with stenosis measurements markedly improves the prediction of both initial and recurrent stroke risk. For instance, Huang et al. [70] showed that among patients with mild to moderate stenosis, those with a Plaque-RADS score of ≥3 (i.e., with plaques at least 3 mm thick) had significantly lower disease-free and recurrence-free survival rates compared to those with lower scores. Wang et al. showed that carotid plaques with Plaque-RADS ≥3 and moderate stenosis had a significantly higher association with symptomatology than those with lower Plaque-RADS scores [71]. By identifying high-risk plaques, clinicians can prioritize patients who may benefit from more aggressive medical therapies or even surgical interventions. This targeted approach is particularly important in asymptomatic individuals, where the presence of a vulnerable plaque may prompt earlier and more intensive management to prevent first-time stroke.

5.2. Intracranial VWI features in stroke patients

ICAD is a major source of morbidity and mortality due to ischemic stroke, accounting for 5–23% of strokes in Caucasians and up to 50% of strokes in East Asians [72,73]. It is often detected in patients presenting with stroke or TIA symptoms, and the asymptomatic incidence is likely higher. Currently, ICAD is primarily detected clinically using luminal imaging such as computed tomographic angiography (CTA), magnetic resonance angiography (MRA), or digital subtraction angiography (DSA) [74]. However, lumen stenosis may be absent or subtle in the setting of positive remodeling. Sun et al. found no association between stenosis measurements and quantitative ICAD maximum wall thickness metrics from 80 ICAD lesions in 24 patients [75]. Non-stenotic ICAD plaques that frequently go undetected on luminal imaging can contribute to ischemic stroke events [40,76]. For example, the strongest predictor of perforator territory infarcts in multivariate regression analysis was non-stenotic plaques along the superior surface of the middle cerebral artery, involving the perforator branch ostia (odds ratio [OR] 28.51, 95% confidence interval 6.34–181.02) [76].

ICAD detection and characterization have been greatly facilitated by the addition of VWI, which has superior tissue contrast compared to CTA [77]. Characteristic findings on all MR VWI contrasts include

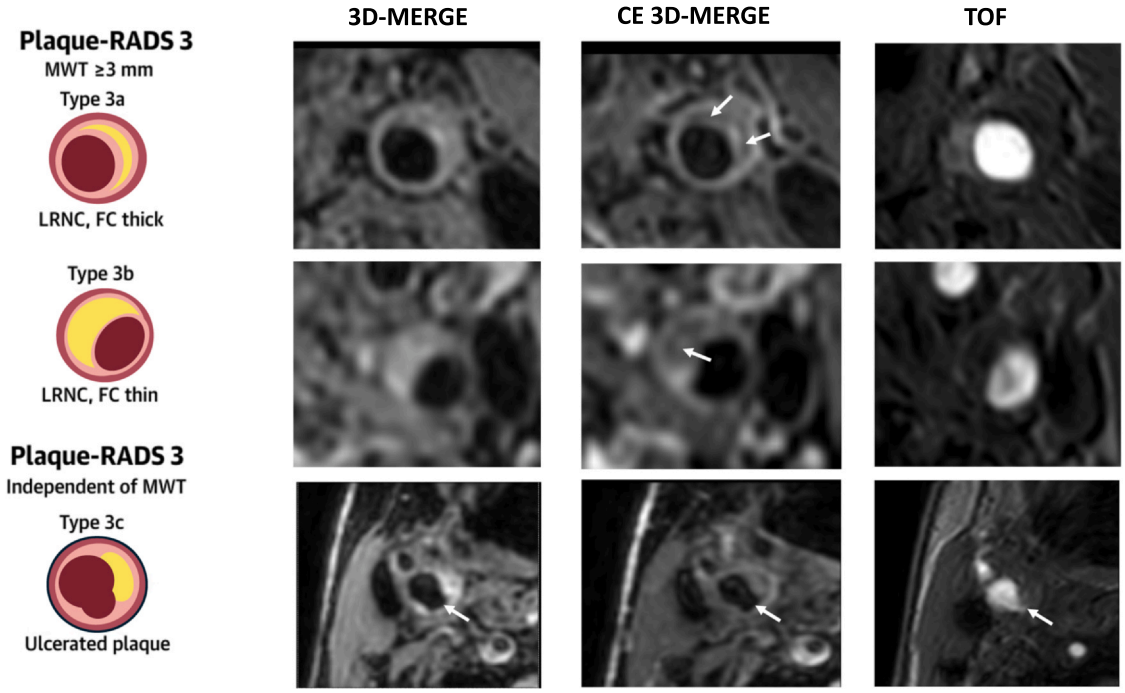

Fig. 4. Panel shows MRI appearance of Plaque-RADS 3 categories. The first column shows a schematic representation of the plaque structure: Dark red—lumen, light pink—fibrous tissue, yellow—lipid-rich necrotic core (LRNC). First row: eccentric plaque with LRNC seen as non-enhancing (arrows) area compared to the pre-contrast scan. The thick fibrous cap is also perceived as a band overlying the LRNC in the CE 3D-MERGE scan and as a dark band on TOF. Second row: an eccentric plaque can be seen on 3D-MERGE with a large non-enhancing LRNC (arrow). There is no dark band overlying the large LRNC on TOF, further indicating a thin fibrous cap. Third row: eccentric plaque with LRNC (2 o'clock position) confirmed by non-enhancement after gadolinium administration is accompanied by ulcer (arrows). The ulcer is clearly seen on 3D-MERGE both pre- and post-contrast and on TOF. *MRI* magnetic resonance imaging, *RADS* Reporting and Data System, *3D* three-dimensional, *3D-MERGE* 3D MSDE prepared rapid gradient echo, *MSDE* motion-sensitized driven equilibrium, *TOF* time-of-flight, *FC* fibrous cap, *MWT* maximal wall thickness, *CE* contrast enhanced.

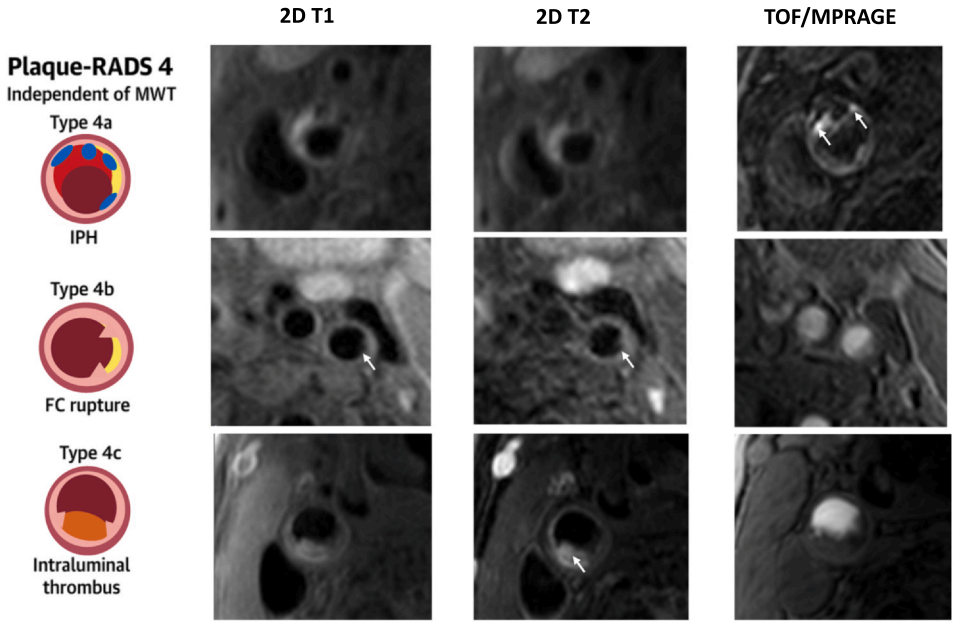

Fig. 5. Panel shows MRI appearance of Plaque-RADS 4 categories. The first column shows a schematic representation of the corresponding plaque structure: Dark red—lumen, light pink—fibrous tissue, yellow—lipid-rich necrotic core (LRNC), bright red—intraplaque hemorrhage, blue—calcification, orange—thrombus. First row: eccentric plaque with several calcifications (seen as hypointense regions on all sequences) also has an IPH seen as hyperintense signal on MPRAGE (arrows). The presence of IPH categorizes this as Plaque-RADS 4a while there is a supplemental designation in Plaque-RADS to denote the additional presence of calcification. Second row: a small surface disruption can be seen on both pre- and post-contrast 3D-MERGE (arrows). The same disruption is seen as luminal protrusion on TOF. Third row: intraluminal thrombus presents as hyperintense luminal protrusion (arrow). *MRI* magnetic resonance imaging, *RADS* Reporting and Data System, *3D* three-dimensional, *3D-MERGE* 3D MSDE prepared rapid gradient echo, *MSDE* motion-sensitized driven equilibrium, *TOF* time-of-flight, *FC* fibrous cap, *MWT* maximal wall thickness, *IPH* intraplaque hemorrhage, *2D* two-dimensional, *MPRAGE* magnetization prepared rapid gradient echo

eccentric wall thickening and progressive lumen narrowing late in disease. Vessel wall enhancement of intracranial arteries after gadolinium injection can provide further diagnostic information. Vessel wall enhancement in ICAD has been found to have a high repeat ischemic stroke risk [78]. It is unknown what causes plaque enhancement in ICAD due to the lack of MRI-compatible animal models and pathology correlation. Possibilities include contrast leakage due to endothelial dysfunction or disruption, or contrast leakage from plaque neovessels associated with plaque inflammation. While vessel wall enhancement has proven useful in identifying vulnerable ICAD, qualitative interpretation of enhancement varies among reviewers. Some advocate for quantitative measurement of post-contrast enhancement to improve inter-rater reliability of VWI findings [79].

Several meta-analyses [80–82] have identified VWI features of intracranial atherosclerosis associated with ischemic stroke, including plaque enhancement [83]. Symptomatic middle cerebral arteries have shown eccentric enhanced lesions, indicative of instability, whereas asymptomatic lesions do not enhance [84]. In fact, a longitudinal study [78] reported a significant difference in event-free survival between patients with enhanced plaques compared to patients without plaque enhancement. A meta-analysis suggests that plaque enhancement is more commonly related to infarction caused by large-artery atherosclerosis than to infarction caused by small-vessel disease [81], which highlights the relevance of VWI in discriminating the subtype of stroke currently considered cryptogenic. Besides plaque enhancement, other features that can be identified using VWI, such as positive remodeling, T1 hyperintensity, and plaque surface irregularity, are features that symptomatic intracranial plaques share in common with symptomatic carotid and coronary atherosclerotic lesions [64,85–87].

ICAD plaque enhancement allows differentiation from stroke mimics such as vasculitis and RCVS [58]. Inflammatory disease leads to concentric enhancement after gadolinium administration and thickening of the intracranial arterial wall. This concentric enhancement and thickening differentiates vasculitis from ICAD, which shows eccentric enhancement and wall thickening [88,89]. Using the same feature, RCVS can be differentiated, where intracranial arterial wall lacks gadolinium enhancement [56].

5.3. VWI and stroke etiology reclassification

Up to one quarter of patients with ischemic stroke have no probable cause identified after standard workup [90,91]. VWI can help with determining stroke etiology in these patients, particularly in strokes of embolic origin [92]. Utilization of VWI results in significant reclassification of stroke etiology, most commonly from undetermined to large-artery atherosclerosis classification [93,94]. In one study, VWI altered the stroke etiologic classification based on the modified Trial of Org 10172 in Acute Stroke Treatment (TOAST) classification in 55% (112/205) of cases [93]. Following clinical guidelines for interpreting VWI [43], Schaafsma et al. [93] evaluated VWI for etiologic classification in patients with recent ischemic stroke or TIA. They used a modified TOAST [95] classification, which included intracranial arterial dissection, vasculitis, RCVS, and unspecified intracranial arteriopathy. The proportion of cases with “unspecified intracranial arteriopathy” decreased from 31% to 4% (64/205 to 9/205) ($p < 0.001$). At the same time, the proportion of cases with “intracranial atherosclerotic disease” increased from 23% to 57% (48/205 to 116/205) ($p < 0.001$). Similar findings were reported for a recent stroke population from India, with greatest impact of VWI on the intracranial atherosclerotic category (increase from 28.6% to 38.8% (14/49 to 19/49)) [96]. In a cohort of 36 patients with recent ischemic stroke and known ≥50% stenosis in the middle cerebral artery disease [97], VWI changed the etiology of 9 (out of 12) ESUS patients to intracranial atherosclerosis [5], vasculitis [3], and partially occlusive thrombus [1] and supported the clinical diagnosis in the remaining 27 cases. In a study of young adults with ischemic stroke or TIA, VWI led to an increase in the proportion of strokes attributed to large-artery atherosclerosis and reduced the proportion of cryptogenic strokes [98]. Besides emphasizing the relevance of VWI in stroke etiological classification, these studies indicate that intracranial atherosclerosis may be a more significant cause of ischemic stroke than previously recognized and highlight VWI’s ability to detect and characterize intracranial atherosclerotic plaques in symptomatic patients [75,97,99,100].

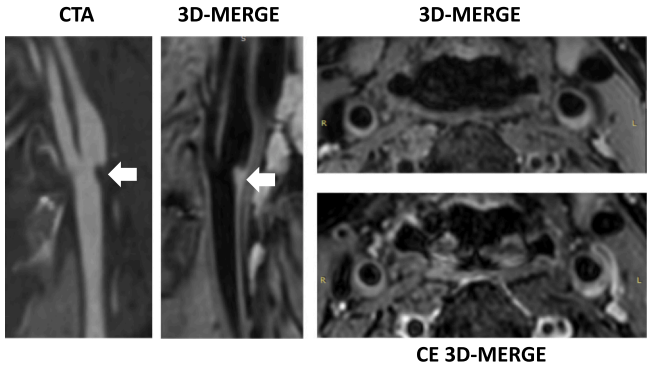

Fig. 6. Carotid web: VWI shows a shelf-like protrusion (arrows) into the lumen corroborated by CTA. Note that there are bilateral carotid webs in this patient, seen on the contralateral carotid in the axial reformat. Gadolinium contrast enhancement is seen at the base of the web on the left carotid on post-contrast 3D-MERGE VWI. *3D* three-dimensional, *3D-MERGE* 3D MSDE prepared rapid gradient echo, *MSDE* motion-sensitized driven equilibrium, *CTA* computed tomographic angiography, *VWI* vessel wall imaging, *CE* contrast enhanced.

6. Other clinical applications of carotid artery VWI

While the majority of carotid VWI is prescribed for the purpose of atherosclerotic plaque characterization, carotid occlusion, webs, and dissections are other clinically important pathologies that benefit from vessel wall MRI. Figs. 6-8 shows carotid web, occlusion, and dissection characteristics by VWI, respectively. In these applications, vessel wall MRI can add additional diagnostic information to clinical angiographic methods such as MRA and CTA.

6.1. Carotid occlusions

There are two main clinical use cases for VWI in the setting of carotid occlusion: to rule out carotid artery pseudo-occlusion and to predict the success of endovascular recanalization of occluded carotids.

While CTA is currently the main non-invasive modality for evaluating carotid occlusions, a distal occlusion such as the carotid T-occlusion or tandem occlusions of the MCA together with severe extracranial carotid stenosis can cause flow stasis in the proximal carotids and lack of contrast opacification, leading to a misdiagnosis of occlusion by CTA [101]. Differentiating pseudo-occlusions from tandem occlusions can help with treatment planning and VWI can play a role in this determination. When comparing VWI to DSA in patients with occlusions by MRA, and determining suitability for recanalization, VWI agreed with DSA in 44.4% (20/45) of cases but VWI found the remaining 25% (11/45) of cases suitable for recanalization in contrast to DSA [102]. While this retrospective study's findings need further corroboration, it shows that the utility of VWI in such recategorization can play an important role in patient management.

VWI can also play a role in the evaluation of occlusions to predict response to recanalization efforts [103]. 3D VWI was found to have excellent agreement with DSA for detecting occlusion site (Cohen's kappa 0.85) and stump morphology (tapered, blunt no stump; Cohen's kappa 0.83) [104]. VWI was found to provide additional information, such as HIS of the distal stump (42.7% (32/75) of occluded stump) corresponding to thrombus/hemorrhage, and evaluate patency of the lumen distal to the occlusion [104]. When proximal stump morphology, extent of occlusion, occlusion with collapse, arterial tortuosity, presence of HIS, and calcification in the occluded C1 segment were evaluated on 3D VWI in patients who had undergone recanalization, a predictive score based on these features showed high predictive value with an area under the curve: 0.89, sensitivity of 0.614, and specificity of 0.962 [105]. Occlusions limited to the C1 segment (OR: 13.84), extensive HIS (OR: 3.99), extensive calcification (OR: 0.19), high tortuosity (OR: 0.12), and artery collapse (OR: 0.20) were significantly associated with successful recanalization after adjustment for clinical factors [105]. Together, these studies illustrate the potential of vessel wall MRI to provide additional value for endovascular treatment planning beyond CTA and DSA in the evaluation of carotid occlusions.

An additional utility of VWI may be in predicting which occlusion may turn out to be symptomatic. The status of the distal end of the occlusion is important to analyze as it may lead to thromboembolism. On VWI, asymptomatic occlusions were isointense while symptomatic occlusions showed hyperintense distal segments [106]. Such hyperintensity may indicate thrombogenic material or inflammation and may require further evaluation/monitoring.

6.2. Carotid webs

A carotid web presents as a shelf or band of fibroelastic tissue on the posterior wall of the carotid artery. Carotid webs have been implicated as a cause of cryptogenic stroke, especially in young patients. While carotid webs may have a low prevalence (1.6% (1/63)) in the general population, there is a high prevalence of carotid webs in the cryptogenic stroke population (21.2% (7/33)) [107]. Owing to their shape and location in the carotid bulb, they may cause turbulent flow and

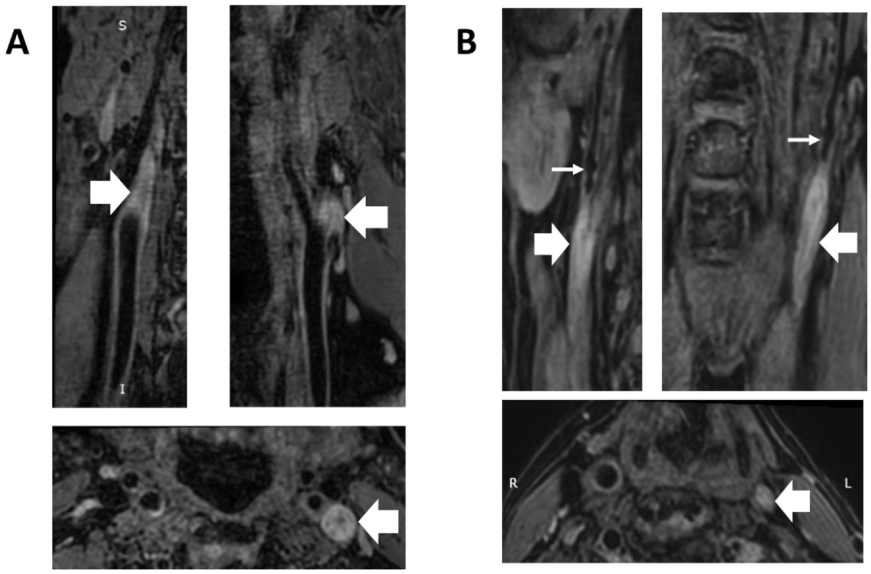

Fig. 7. Chronic carotid occlusion: sagittal, coronal, and axial reformats of two cases of carotid occlusion are shown. (A) Occlusion of the left internal carotid artery on 3D-MERGE shows blunt stump of the occlusion and the hyperintense thrombus (large arrow) within the lumen. (B) Occlusion of the left common carotid and bifurcation in another subject is seen with hyperintense thrombus (large arrow) in the lumen. The distal lumen in the left external carotid artery is patent (small arrow). *3D* three-dimensional, *3D-MERGE* 3D MSDE prepared rapid gradient echo, *MSDE* motion-sensitized driven equilibrium

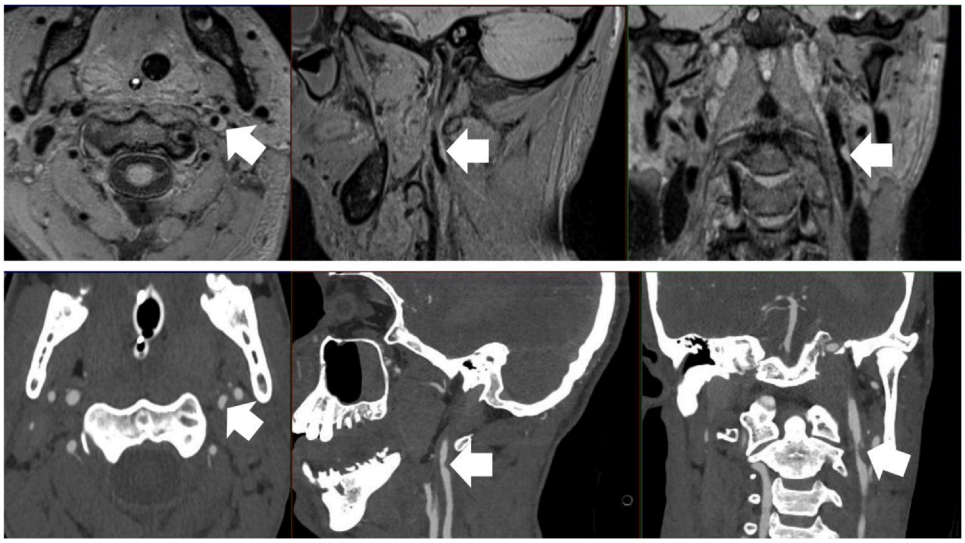

Fig. 8. Carotid dissection: axial view shows eccentric thickening. An occlusion is diagnosed by long hyperintense thickening of the wall best seen in the sagittal VWI as opposed to focal wall thickening of atherosclerosis. The hyperintense signal is also characteristic denoting thrombus/hemorrhage in the false lumen. Corresponding CTA images (bottom row) show similar indentation of the lumen. *CTA* computed tomographic angiography

raise the risk of thromboembolism. While a survey of practicing physicians found that invasive DSA is the most common modality used to confirm carotid webs, some neuroradiologists and neurointerventionalists preferred VWI for follow-up imaging in recurrent stroke [108]. Carotid webs on VWI can be seen as protrusions into the lumen on oblique coronal view, similar to DSA or CTA, and appear as a triangular shelf on axial VWI [109]. Vessel wall enhancement may be present on the post-gadolinium VWI on the side of the carotid web [110]. Given the young age of stroke patients with carotid webs, endarterectomy is preferred for its long-term treatment durability, but stenting can also be performed [111]. Considering the invasive nature of both treatments and the need for long-term monitoring in these patients, MR VWI may be preferable for pre-operative assessment and post-operative follow-up.

6.3. Carotid dissections

Cervical carotid artery dissections can arise in various settings, including major or minor trauma [112,113]. Spontaneous carotid dissection typically results from minor injuries, including sneezing, or in the setting of connective tissue disorders or underlying genetic disorders [113]. Dissections may present either as an intramural hematoma with luminal narrowing or as a dissection flap with false lumen. Thrombosis of the false lumen may present as T1 HIS in the subacute phase, similar to IPH, however, may be T1 isointense and T2 HIS in the acute phase [114]. Dissections may also manifest as a pseudoaneurysm with or without surrounding soft tissue hemorrhage. While dissections are mostly distal to the carotid bifurcation, atherosclerotic IPH is mostly centered around the carotid bifurcation. The presence of other atherosclerotic plaque components or wall thickening strongly suggests atherosclerosis-related thrombus/hematoma in contrast to dissection. Acute unilateral pain accompanies dissection [115] and VWI can aid in improved diagnosis. While thrombus/hematoma has been described using sequences such as 2D T1 or PD weighted sequences as well as 3D SPACE/VISTA/CUBE, the highly T1-weighted sequences, SNAP, and MPRAGE with demonstrated ability to identify IPH, have been shown to be useful for cervical dissections with higher signal or contrast for intramural hematoma [116, 117]. VWI characteristics in craniocervical arterial dissection, specifically lumen surface irregularity and intraluminal thrombus, showed significant independent associations with acute stroke on multivariable regression analysis [118].

Blunt cerebrovascular injury (BCVI) is a dissection that develops in the setting of acute blunt force trauma to the neck. While historically considered rare, BCVI has increased to 1–3% prevalence in trauma cohorts, likely due to increased and improved diagnostic cross-sectional imaging [112]. BCVI is associated with a delayed stroke risk of 4.7% (54/1146) across all grade injuries [119]; however, this risk increased with higher grade injuries, transcranial Doppler evidence of embolization, carotid artery injuries, or multiple arterial injuries, as did the risk of arterial injury progression [120]. Without appropriate treatment, the stroke risk is substantially increased as well [121]. BCVI imaging characteristics mirror those of arterial dissection on VWI [112]. Vranic et al. compared CTA and VWI evaluation of BCVI relative to expert clinical consensus as the reference standard and found that VWI was more accurate for accurate BCVI detection, which was most appreciated for CTA suspected low-grade or indeterminate injuries [122]. With indeterminate BCVI, the utilization of VWI may confirm the lack of arterial injury and lead to shortened hospital stays, reduced medication, follow-up imaging, and follow-up outpatient evaluations, thus reducing patient risk and health care costs.

7. Other clinical applications of intracranial VWI

7.1. Intracranial vasculopathy differentiation

VWI has shown the ability to differentiate intracranial vasculopathies through multi-contrast protocols [51], and vasculopathy differentiation was the most common reason for clinical application of intracranial VWI [12]. Intracranial VWI can differentiate ICAD from other pathologies such as vasculitis, moyamoya vasculopathies, and RCVS. VWI improved diagnostic accuracy for non-occlusive intracranial vasculopathies (including ICAD, vasculitis, and RCVS) from 36% (145/402) using luminal imaging to 89% (357/402) on a per-lesion basis, with significant diagnostic accuracy improvement for each disease state [57]. Use of VWI for vasculopathy differentiation is therefore of added clinical benefit to traditional luminal imaging.

7.1.1. Vasculitis differentiation

Inflammatory vasculopathies such as vasculitis typically show circumferential intense wall enhancement with an isointense T2-weighted signal relative to gray matter. Inflammatory vasculopathies also cause perivascular inflammatory changes, resulting in a more pronounced halo of enhancement that frequently has irregular or fuzzy margins, unlike the clearly defined outer wall appreciated with ICAD. These features help differentiate ICAD which most commonly shows eccentric wall enhancement with outward remodeling, heterogeneous and variable enhancement, and juxtaluminal T2 hyperintensity with central

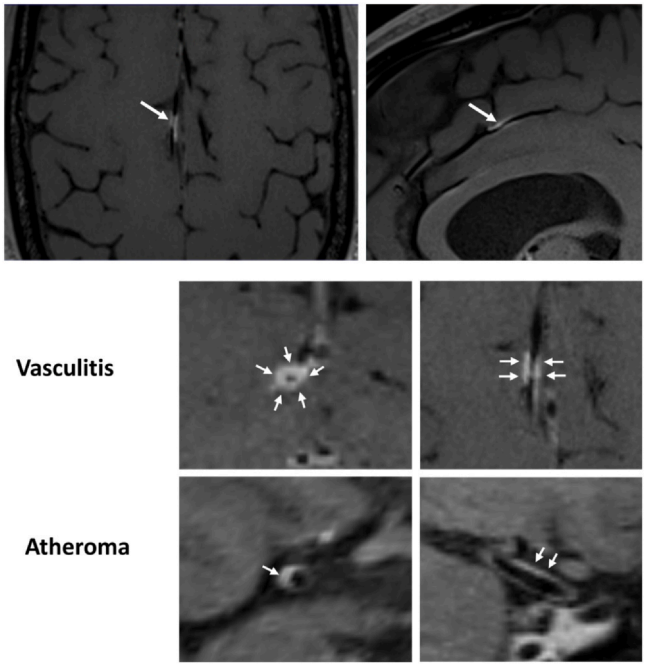

Fig. 9. Top row shows a case of vasculitis of the right anterior cerebral artery with post-gadolinium enhancement (arrows). Bottom two rows show how vasculitis can be differentiated from atherosclerosis. Vasculitis shows concentric wall enhancement in affected areas with accompanying circumferential wall thickening without significant eccentricity (middle row) in contrast to atherosclerosis (bottom row) where the wall enhancement is eccentric.

hypointensity. Fig. 9 shows an example of vasculitis and its differentiation from ICAD.

7.1.2. RCVS differentiation

RCVS presents as stenosis on luminal angiography, but it can be differentiated from ICAD using VWI. RCVS represents a non-inflammatory process with vasospasm resulting from sympathetic system stimulation, and thus the disease process may show minimal to no wall enhancement, imperceptible wall thickening, and no appreciable T2-weighted wall signal abnormality. Fig. 10 shows an example of RCVS. RCVS can cause multi-compartmental intracranial hemorrhage, including subarachnoid hemorrhage that contributes to inflammation and may sometimes cause arterial wall enhancement. However, the degree of enhancement is lower and without wall thickening seen in inflammatory vasculopathies and ICAD [51]. Combining VWI features with cerebrospinal fluid pleocytosis, patient presentation of encephalopathy and/or headache significantly improves the discrimination of primary vasculitis from ICAD [88].

7.1.3. Moyamoya differentiation

The intracranial vessel wall in patients with Moyamoya vasculopathy is generally characterized by concentric enhancement, with enhancement often found in the distal intracranial internal carotid artery [123,124]. VWI improved the diagnostic accuracy for moyamoya vasculopathies over luminal imaging (32% (24/76) to 87% (66/76)) [50]. Similarly, traditional luminal measures for Moyamoya disease diagnosis, including extensive collaterals, did not show any significant differentiation capacity from ICAD Moyamoya syndrome.

7.2. Assessment of unruptured aneurysms

VWI for aneurysm assessment is an active area of investigation, and several studies have addressed the utility of VWI for aneurysm wall evaluation [125–127]. Qualitative assessment of aneurysms using VWI can also predict complications such as aneurysmal subarachnoid hemorrhage [54,128]. In 22 ruptured aneurysm cases, arterial wall enhancement on post-intervention VWI showed a significant association with the development of angiographic vasospasm while controlling for hemorrhage grade (OR 3.9, 95% CI 1.7–9.4) [54]. Aneurysmal wall enhancement has also shown a significant association with delayed cerebral ischemia in 32 ruptured cases ($p < 0.04$) [128].

8. Future of VWI and summary

Despite the progress in clinical application of VWI, there are existing challenges to widespread use of MR VWI that must be overcome to accelerate clinical adoption: 1) lack of reimbursement for VWI: while VWI has been shown to benefit clinical diagnosis in multiple pathologies, use of VWI is not mandated by clinical guidelines. If clinical guidelines are set forth for VWI, followed by reimbursement of VWI scans, then utilization of VWI is expected to increase exponentially, considering its demonstrated clinical utility and demand from clinicians. 2) Limited training in VWI: current use of VWI is limited to research institutions with the expertise to conduct and interpret VWI scans. As noted by the ASNR surveys [11, 12], lack of training in clinical applications and image interpretation is a major limitation to the use of VWI. Adding training on VWI applications and image interpretation to medical curricula and continued medical education settings, as well as active outreach to practicing physicians, may help to resolve this limitation. 3) Lack of commercial VWI analysis products: there are few established VWI analysis products that are clinically usable. Commercialization of tailored VWI analysis and reporting methods can expand clinical use. Provisioning reimbursement pathways for VWI will also foster more commercialization ventures and

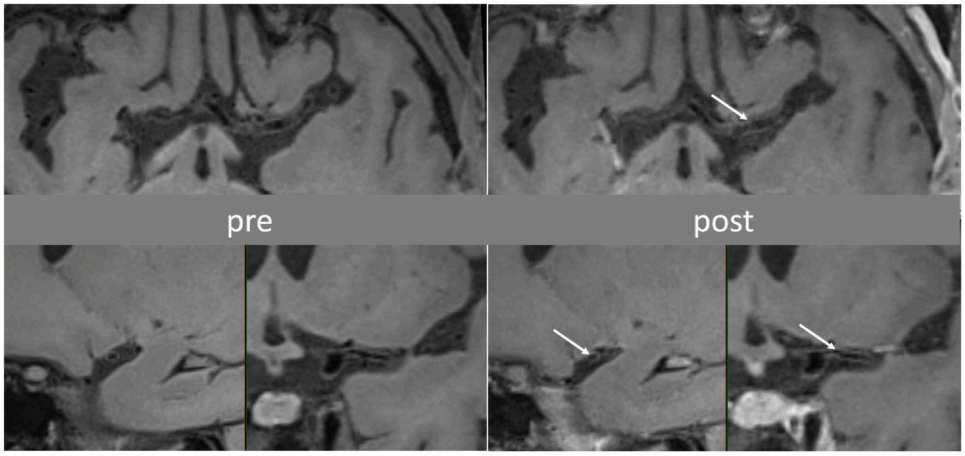

Fig. 10. Pre- and post-gadolinium contrast VWI images of a case of reversible cerebral vasoconstriction syndrome of the left middle cerebral artery are shown in axial, sagittal, and coronal views. Vessel wall imaging shows narrowing of left MCA (arrow) but without appreciable wall thickening or enhancement. *VWI* vessel wall imaging, *MCA* middle cerebral artery

further drive clinical use. 4) Standardized reporting of VWI is lacking: a consensus is required on what are the essential features of VWI that should be clinically reported. Introduction of the Plaque-RADS scoring system is a promising step in this direction. With increased validation of Plaque-RADS in the clinical setting, it may provide the much-needed structure for clinical VWI reporting. For both carotid and intracranial VWI, there remains a need for streamlined and efficient imaging techniques with shorter standardized protocols distributed by the major MRI vendors and development of automated quantitative post-processing tools to facilitate quicker evaluation and more reproducible imaging analysis that will facilitate a shorter radiologist learning curve and easier clinical adoption. With AI playing a key role in the advancement of imaging technology, it is foreseeable that it may also help in VWI in terms of image acquisition efficiency, quality, imaging analysis, and quantitation methods. Some interesting works are already being reported [129,130].

On the other hand, computed tomography (CT) VWI is emerging as an alternative to MR VWI [131–133]. CT VWI is attractive in terms of ease of use and availability. Carotid plaque volume, calcification, and ulceration can be reliably identified on CT [132], while LRNC and IPH may also be detected [131, 132]. CT is preferable for the identification of calcifications and ulcerations. However, the role of CT in identifying non-calcified intracranial plaque is not clear. Currently, MR VWI has the advantage in detecting IPH. Hence, MR VWI may be preferable for high-risk carotid component detection and for intracranial plaque detection. It is important to consider the strengths and limitations of both CT and MRI when optimizing clinical VWI workflow. There may be a need to include both, depending upon clinical needs.

An untapped clinical role of VWI is in CV disease prevention [43, 134]. Early changes in the vessel wall may be identified by VWI, offering unique opportunities for early detection of systemic vascular disease by targeting certain vascular beds, such as the carotid. Considering the extensive clinical benefits of VWI, the possibility of including VWI as part of future diagnosis, monitoring, and treatment planning guidelines should be considered. Future incorporation of VWI into clinical guidelines will require the concerted effort of clinicians to design imaging trials based on the current knowledge and practice of MR VWI.

Author contributions

Chun Yuan: Writing – review & editing, Writing – original draft, Conceptualization. **Thomas Hatsukami:** Writing – review & editing. **Scott McNally:** Writing – review & editing, Writing – original draft. **Luca Saba:** Writing – review & editing, Writing – original draft. **Mahmud Mossa-Basha:** Writing – review & editing, Writing – original draft. **Gador Canton:** Writing – review & editing, Writing – original draft. **Niranjan Balu:** Writing – review & editing, Writing – original draft, Conceptualization.

Declaration of competing interests

The authors declare that they have no known competing financial interests or personal relationships that could have appeared to influence the work reported in this paper.

Acknowledgements

The authors acknowledge Drs. Mona Kharaji, Cristina Sanchez-Vizcaino, and Beibei Sun for their assistance in preparing figures.

References

[1] Chu B, Kampschulte A, Ferguson MS, Kerwin WS, Yarnykh VL, O'Brien KD, et al. Hemorrhage in the atherosclerotic carotid plaque: a high-resolution MRI study. Stroke 2004;35(5):1079–84.
[2] Kampschulte A, Ferguson MS, Kerwin WS. Differentiation of intraplaque versus juxtaluminal hemorrhage/thrombus in advanced human carotid atherosclerotic lesions by in vivo magnetic resonance imaging. Circulation 2004;110:3239–44.
[3] Wasserman BA, Smith WI. Trout 3rd HH, Cannon 3rd RO, Balaban RS, Arai AE. Carotid artery atherosclerosis: in vivo morphologic characterization with gadolinium-enhanced double-oblique MR imaging initial results. Radiology 2002;223(2):566–73.
[4] Yuan C, Kerwin WS, Ferguson MS, Polissar N, Zhang S, Cai J, et al. Contrast-enhanced high resolution MRI for atherosclerotic carotid artery tissue characterization. J Magn Reson Imaging 2002;15(1):62–7. https://doi.org/10.1002/jmri.10030%2520%255Bpii%255D.
[5] Takaya N, Cai J, Ferguson MS, Yarnykh VL, Chu B, Saam T, et al. Intra- and interreader reproducibility of magnetic resonance imaging for quantifying the lipid-rich necrotic core is improved with gadolinium contrast enhancement. J Magn Reson Imaging. 2006;24:203–10. https://doi.org/10.1002/jmri.20599.
[6] Saam T, Ferguson MS, Yarnykh VL. Quantitative evaluation of carotid plaque composition by in vivo MRI. Arterioscler Thromb Vasc Biol 2004;25:234–9.
[7] Yuan C, Zhang S, Polissar NL, Echelard D, Ortiz G, Davis JW, et al. Identification of fibrous cap rupture with magnetic resonance imaging is highly associated with recent transient ischemic attack or stroke. Circulation 2002;105:181–5. https://doi.org/10.1161/hc0202.102121.
[8] Schindler A, Schinner R, Altaf N. Prediction of Stroke Risk by Detection of Hemorrhage in Carotid Plaques: Meta-Analysis of Individual Patient Data. JACC Cardiovasc Imaging 2020;13:395–406.
[9] Altaf N, MacSweeney ST, Gladman J, Auer DP. Carotid intraplaque hemorrhage predicts recurrent symptoms in patients with high-grade carotid stenosis. STROKE. 2007;38:1633–5.
[10] Takaya N, Yuan C, Chu B. Presence of intraplaque hemorrhage stimulates progression of carotid atherosclerotic plaques - A high-resolution magnetic resonance Imaging study. CIRCULATION 2005;111:2768–75.
[11] Mossa-Basha M, Yuan C, Wasserman BA, Mikulis DJ, Hatsukami TS, Balu N, et al. Survey of the American Society of Neuroradiology Membership on the Use and Value of Extracranial Carotid Vessel Wall MRI. AJNR Am J Neuroradiol 2022;43:1756–61. https://doi.org/10.3174/ajnr.A7720.
[12] Mossa-Basha M, Zhu C, Yuan C, Saba L, Saloner DA, Edjlali M, et al. Survey of the American Society of Neuroradiology Membership on the Use and Value of Intracranial Vessel Wall MRI. AJNR Am J Neuroradiol 2022;43:951–7. https://doi.org/10.3174/ajnr.A7541.
[13] Yuan C, Murakami JW, Hayes CE, Tsuruda JS, Hatsukami TS, Wildy KS, et al. Phased-array magnetic resonance imaging of the carotid artery bifurcation: preliminary results in healthy volunteers and a patient with atherosclerotic disease. J Magn Reson Imaging 1995;5(5):561–5.
[14] Hayes CE, Mathis CM, Yuan C. Surface coil phased arrays for high-resolution imaging of the carotid arteries. J Magn Reson Imaging 1996;6(1):109–12.
[15] Saba L, Yuan C, Hatsukami TS, Balu N, Qiao Y, DeMarco JK, et al. Carotid Artery Wall Imaging: Perspective and Guidelines from the ASNR Vessel Wall Imaging Study Group and Expert Consensus Recommendations of the American Society of Neuroradiology. AJNR Am J Neuroradiol 2018;39:E9–31. https://doi.org/10.3174/ajnr.A5488.
[16] Balu N, Yarnykh VL, Scholnick J, Chu B, Yuan C, Hayes C. Improvements in carotid plaque imaging using a new eight-element phased array coil at 3T. J Magn Reson Imaging 2009;30(5):1209–14. https://doi.org/10.1002/jmri.21890.
[17] Beck MJ, Parker DL, Bolster BD, Kim S-E, McNally JS, Treiman GS, et al. Interchangeable neck shape-specific coils for a clinically realizable anterior neck phased array system. Magn Reson Med 2017;78:2460–8. https://doi.org/10.1002/mrm.26632.
[18] Zhang Q, Coolen BF, Van Den Berg S, Kotek G, Rivera DS, Klomp DWJ, et al. Comparison of four MR carotid surface coils at 3T. In: Jiang Q, editor. PLoS ONE, 14. 2019:e0213107. https://doi.org/10.1371/journal.pone.0213107.
[19] De Buck MHS, Jezzard P, Frost R, Randell C, Hurst K, Choudhury RP, et al. 10-channel phased-array coil for carotid wall MRI at 3T. In: Orzada S, editor. PLoS ONE, 18. 2023:e0288529. https://doi.org/10.1371/journal.pone.0288529.
[20] Koktzoglou I, Li D. Diffusion-prepared segmented steady-state free precession: Application to 3D black-blood cardiovascular magnetic resonance of the thoracic aorta and carotid artery walls. J Cardiovasc Magn Reson 2007;9(1):33–42. https://doi.org/X62575X231G02776%2520%255Bpii%255D%252010.1080/10976640600843413.
[21] Wang J, Yarnykh V, Hatsukami T, Chu B, Balu N, Yuan C. Improved suppression of plaque-mimicking artifacts in black-blood carotid atherosclerosis imaging using a multislice motion-sensitized driven-equilibrium (MSDE) turbo spin-echo (TSE) sequence. MAGNETIC RESONANCE IN MEDICINE 2007;58(5):973–81.
[22] Li L, Miller KL, Jezzard P. DANTE-prepared pulse trains: a novel approach to motion-sensitized and motion-suppressed quantitative magnetic resonance imaging. Magn Reson Med 2012;68:1423–38.
[23] Balu N, Yarnykh VL, Chu B, Wang J, Hatsukami T, Yuan C. Carotid plaque assessment using fast 3D isotropic resolution black-blood MRI. Magn Reson Med 2011;65:627–37. https://doi.org/10.1002/mrm.22642.
[24] Fan Z, Zhang Z, Chung Y, Weale P, Zuehlsdorff S, Carr J, et al. Carotid arterial wall MRI at 3T using 3D variable-flip-angle turbo spin-echo (TSE) with flow-sensitive dephasing (FSD. Magnetic Resonance Imaging 2010;31:645–54. https://doi.org/10.1002/jmri.22058.
[25] Brinjikji W, DeMarco JK, Shih R, Lanzino G, Rabinstein AA, Hilditch CA, et al. Diagnostic accuracy of a clinical carotid plaque MR protocol using a neurovascular coil compared to a surface coil protocol. Magnetic Resonance Imaging 2018;48:1264–72. https://doi.org/10.1002/jmri.25984.

[26] Cai J-M, Hatsukami TS, Ferguson MS, Small R, Polissar NL, Yuan C. Classification of human carotid atherosclerotic lesions with in vivo multicontrast magnetic resonance imaging. Circulation 2002;106:1368–73. https://doi.org/10.1161/01.cir.0000028591.44554.f9.

[27] Edelman RR, Chien D, Kim D. Fast selective black blood MR imaging. Radiology 1991;181(3):655–60.

[28] Yarnykh VL, Yuan C. Multislice double inversion-recovery black-blood imaging with simultaneous slice reinversion. J Magn Reson Imaging 2003;7(4):478–83. https://doi.org/10.1002/jmri.10278.

[29] Mugler JP. Optimized three-dimensional fast-spin-echo MRI. Magnetic Resonance Imaging 2014;39:745–67. https://doi.org/10.1002/jmri.24542.

[30] Qiao Y, Steinman DA, Qin Q, Etesami M, Schar M, Astor BC, et al. Intracranial arterial wall imaging using three-dimensional high isotropic resolution black blood MRI at 3.0 Tesla. J Magn Reson Imaging 2011;34(1):22–30. https://doi.org/10.1002/jmri.22592. %252010.1002/jmri.22592.

[31] Edjlali M, Roca P, Rabrait C, Naggara O, Oppenheim C. 3D Fast Spin-Echo T1 Black-Blood Imaging for the Diagnosis of Cervical Artery Dissection. AJNR Am J Neuroradiol 2013;34:E103–6. https://doi.org/10.3174/ajnr.A3261.

[32] Li Y, Chen Q, Wei Z, Zhang L, Tie C, Zhu Y, et al. One-stop MR neurovascular vessel wall imaging with a 48-channel coil system at 3 T. IEEE Trans Biomed Eng 2020;67(8):2317–27. https://doi.org/10.1109/TBME.2019.2959030.

[33] Li L, Chai JT, Biasiolli L, Robson MD, Choudhury RP, Handa AI, et al. Black-blood multicontrast imaging of carotid arteries with DANTE-prepared 2D and 3D MR imaging. Radiology 2014;273(2):560–9. https://doi.org/10.1148/radiol.14131717.

[34] Moody AR. Magnetic resonance direct thrombus imaging. J Thromb Haemost 2003;1(7):1403–9.

[35] Wang J, Börnert P, Zhao H, Hippe DS, Zhao X, Balu N, et al. Simultaneous non-contrast angiography and intraPlaque hemorrhage (SNAP) imaging for carotid atherosclerotic disease evaluation. Magn Reson Med 2013;69:337–45. https://doi.org/10.1002/mrm.24254.

[36] Fan Z, Yu W, Xie Y, Dong L, Yang L, Wang Z, et al. Multi-contrast atherosclerosis characterization (MATCH) of carotid plaque with a single 5-min scan: technical development and clinical feasibility. 5 J Cardiovasc Magn Reson 2014;16(1):53. https://doi.org/10.1186/s12968-014-0053-5.

[37] Toussaint JF, LaMuraglia GM, Southern JF, Fuster V, Kantor HL. Magnetic resonance images lipid, fibrous, calcified, hemorrhagic, and thrombotic components of human atherosclerosis in vivo. Circulation 1996;94(5):932–8.

[38] Yuan C, Kerwin WS, Ferguson MS. Contrast-enhanced high resolution MRI for atherosclerotic carotid artery tissue characterization. JOURNAL OF MAGNETIC RESONANCE IMAGING 2002;15:62–7.

[39] Yarnykh VL, Yuan C. T1-insensitive flow suppression using quadruple inversion-recovery. Magn Reson Med 2002;48:899–905. https://doi.org/10.1002/mrm.10292.

[40] de Havenon A, Yuan C, Tirschwell D, Hatsukami T, Anzai Y, Becker K, et al. Nonstenotic Culprit Plaque: The Utility of High-Resolution Vessel Wall MRI of Intracranial Vessels after Ischemic Stroke. Case Rep Radiol 2015;2015:356582. https://doi.org/10.1155/2015/356582.

[41] Sannananja B, Zhu C, Colip CG, Somasundaram A, Ibrahim M, Khrisat T, et al. Image-Quality Assessment of 3D Intracranial Vessel Wall MRI Using DANTE or DANTE-CAIPI for Blood Suppression and Imaging Acceleration. AJNR Am J Neuroradiol 2022;43:837–43. https://doi.org/10.3174/ajnr.A7531.

[42] Kharaji M, Canton G, Guo Y, Mosi MH, Zhou Z, Balu N, et al. DANTE-CAIPI Accelerated Contrast-Enhanced 3D T1: Deep Learning-Based Image Quality Improvement for Vessel Wall MRI. AJNR Am J Neuroradiol 2025;46:49–56. https://doi.org/10.3174/ajnr.A8424.

[43] Mandell DM, Mossa-Basha M, Qiao Y, Hess CP, Hui F, Matouk C, et al. Intracranial Vessel Wall MRI: Principles and Expert Consensus Recommendations of the American Society of Neuroradiology. AJNR Am J Neuroradiol 2017;38:218–29. https://doi.org/10.3174/ajnr.A4893.

[44] Balu N, Zhou Z, Hippe DS, Hatsukami T, Mossa-Basha M, Yuan C. Accelerated multi-contrast high isotropic resolution 3D intracranial vessel wall MRI using a tailored k-space undersampling and partially parallel reconstruction strategy. MAGMA. 2019;32:343–57. https://doi.org/10.1007/s10334-018-0730-8.

[45] Jia S, Zhang L, Ren L, Qi Y, Ly J, Zhang N, et al. Joint intracranial and carotid vessel wall imaging in 5 minutes using compressed sensing accelerated DANTE-SPACE. Eur Radiol 2020;30:119–27. https://doi.org/10.1007/s00330-019-06366-7.

[46] Vranic JE, Cross NM, Wang Y, Hippe DS, de Weerdt E, Mossa-Basha M. Compressed Sensing-Sensitivity Encoding (CS-SENSE) Accelerated Brain Imaging: Reduced Scan Time without Reduced Image Quality. AJNR Am J Neuroradiol 2019;40:92–8. https://doi.org/10.3174/ajnr.A5905.

[47] Bathla G, Messina SA, Black DF, Benson JC, Kollasch P, Nickel MD, et al. Deep Learning-Based Reconstruction of 3D T1 SPACE Vessel Wall Imaging Provides Improved Image Quality with Reduced Scan Times: A Preliminary Study. AJNR Am J Neuroradiol 2024;45:1655–60. https://doi.org/10.3174/ajnr.A8382.

[48] Ota H, Yarnykh V, Ferguson M, Underhill H, Demarco J, Zhu D, et al. Carotid intraplaque hemorrhage imaging at 3.0-T MR imaging: comparison of the diagnostic performance of three T1-weighted sequences. Radiology 2010;254(2):551–63.

[49] Aoki S, Shirouzu I, Sasaki Y, Okubo T, Hayashi N, Machida T, et al. Enhancement of the intracranial arterial wall at MR imaging: relationship to cerebral atherosclerosis. Radiology 1995;194(2):477–81. https://doi.org/10.1148/radiology.194.2.7824729.

[50] Mossa-Basha M, de Havenon A, Becker KJ, Hallam DK, Levitt MR, Cohen WA, et al. Added Value of Vessel Wall Magnetic Resonance Imaging in the Differentiation of Moyamoya Vasculopathies in a Non-Asian Cohort. Stroke 2016;47:1782–8. https://doi.org/10.1161/STROKEAHA.116.013320.

[51] Mossa-Basha M, Hwang WD, De Havenon A, Hippe D, Balu N, Becker KJ, et al. Multicontrast high-resolution vessel wall magnetic resonance imaging and its value in differentiating intracranial vasculopathic processes. Stroke 2015;46:1567–73. https://doi.org/10.1161/STROKEAHA.115.009037.

[52] Hartman JB, Watase H, Sun J, Hippe DS, Kim L, Levitt M, et al. Intracranial aneurysms at higher clinical risk for rupture demonstrate increased wall enhancement and thinning on multicontrast 3D vessel wall MRI. Br J Radiol 2019;92(1096):20180950. https://doi.org/10.1259/bjr.20180950.

[53] Guo Y, Canton G, Baylam Geleri D, Balu N, Sun J, Kharaji M, et al. Plaque Evolution and Vessel Wall Remodeling of Intracranial Arteries: A Prospective, Longitudinal Vessel Wall MRI Study. J Magn Reson Imaging 2024;60:889–99. https://doi.org/10.1002/jmri.29185.

[54] Mossa-Basha M, Huynh TJ, Hippe DS, Fata P, Morton RP, Levitt MR. Vessel wall MRI characteristics of endovascularly treated aneurysms: association with angiographic vasospasm. J Neurosurg 2019;131:859–67. https://doi.org/10.3171/2018.4.JNS172829.

[55] Sannananja B, Zhu C, Mossa-Basha M. Vessel Wall Imaging in Cryptogenic Stroke. Radiol Clin North Am 2023;61:491–500. https://doi.org/10.1016/j.rcl.2023.01.006.

[56] Mandell DM, Matouk CC, Farb RI, Krings T, Agid R, terBrugge K, et al. Vessel wall MRI to differentiate between reversible cerebral vasoconstriction syndrome and central nervous system vasculitis: preliminary results. Stroke 2012;43(3):860–2. https://doi.org/10.1161/STROKEAHA.111.626184.

[57] Mossa-Basha M, Shibata DK, Hallam DK. Added Value of Vessel Wall Magnetic Resonance Imaging for Differentiation of Nonocclusive Intracranial Vasculopathies. Stroke 2017;48:3026–33.

[58] Swartz RH, Bhuta SS, Farb RI, Agid R, Willinsky RA, Terbrugge KG, et al. Intracranial arterial wall imaging using high-resolution 3-tesla contrast-enhanced MRI. 17 Neurology 2009;72(7):627–34. https://doi.org/10.1212/01.wnl.0000342470.69739.b3. %252010.1212/01.wnl.0000342470.69739.b3.

[59] Ntaios G, Swaminathan B, Berkowitz SD, Gagliardi RJ, Lang W, Siegler JE, et al. Efficacy and Safety of Rivaroxaban Versus Aspirin in Embolic Stroke of Undetermined Source and Carotid Atherosclerosis. Stroke 2019;50:2477–85. https://doi.org/10.1161/STROKEAHA.119.025168.

[60] Coutinho JM, Derkatch S, Potvin ARJ, Tomlinson G, Kiehl T-R, Silver FL, et al. Nonstenotic carotid plaque on CT angiography in patients with cryptogenic stroke. Neurology 2016;87:665–72. https://doi.org/10.1212/WNL.0000000000002978.

[61] Ospel JM, Singh N, Marko M, Almekhlafi M, Dowlatshahi D, Puig J, et al. Prevalence of Ipsilateral Nonstenotic Carotid Plaques on Computed Tomography Angiography in Embolic Stroke of Undetermined Source. Stroke 2020;51:1743–9. https://doi.org/10.1161/STROKEAHA.120.029404.

[62] Freilinger TM, Schindler A, Schmidt C, Grimm J, Cyran C, Schwarz F, et al. Prevalence of nonstenosing, complicated atherosclerotic plaques in cryptogenic stroke. JACC Cardiovasc Imaging 2012;5:397–405. https://doi.org/10.1016/j.jcmg.2012.01.012.

[63] Kamel H, Navi BB, Merkler AE, Baradaran H, Díaz I, Parikh NS, et al. Reclassification of Ischemic Stroke Etiological Subtypes on the Basis of High-Risk Nonstenosing Carotid Plaque. Stroke 2020;51:504–10. https://doi.org/10.1161/STROKEAHA.119.027970.

[64] Zhao X, Hippe DS, Li R, Canton GM, Sui B, Song Y, et al. Prevalence and Characteristics of Carotid Artery High-Risk Atherosclerotic Plaques in Chinese Patients With Cerebrovascular Symptoms: A Chinese Atherosclerosis Risk Evaluation II Study. J Am Heart Assoc 2017;6:e005831. https://doi.org/10.1161/JAHA.117.005831.

[65] Kopczak A, Schindler A, Bayer-Karpinska A, Koch ML, Sepp D, Zeller J, et al. Complicated Carotid Artery Plaques as a Cause of Cryptogenic Stroke. J Am Coll Cardiol 2020;76:2212–22. https://doi.org/10.1016/j.jacc.2020.09.532.

[66] Gupta A, Gialdini G, Lerario MP, Baradaran H, Giambrone A, Navi BB, et al. Magnetic resonance angiography detection of abnormal carotid artery plaque in patients with cryptogenic stroke. J Am Heart Assoc 2015;4:e002012. https://doi.org/10.1161/JAHA.115.002012.

[67] Gupta A, Gialdini G, Giambrone AE, Lerario MP, Baradaran H, Navi BB, et al. Association Between Nonstenosing Carotid Artery Plaque on MR Angiography and Acute Ischemic Stroke. JACC Cardiovasc Imaging 2016;9:1228–9. https://doi.org/10.1016/j.jcmg.2015.12.004.

[68] Singh N, Moody AR, Panzov V, Gladstone DJ. Carotid Intraplaque Hemorrhage in Patients with Embolic Stroke of Undetermined Source. J Stroke Cerebrovasc Dis 2018;27:1956–9. https://doi.org/10.1016/j.jstrokecerebrovasdis.2018.02.042.

[69] Saba L, Cau R, Murgia A, Nicolaides AN, Wintermark M, Castillo M, et al. Carotid Plaque-RADS: A Novel Stroke Risk Classification System. JACC Cardiovasc Imaging 2024;17:62–75. https://doi.org/10.1016/j.jcmg.2023.09.005.

[70] Huang Z, Cheng X-Q, Lu R-R, Bi X-J, Liu Y-N, Deng Y-B. Incremental Prognostic Value of Carotid Plaque-RADS Over Stenosis Degree in Relation to Stroke Risk. JACC Cardiovasc Imaging 2025;18:77–89. https://doi.org/10.1016/j.jcmg.2024.07.004.

[71] Wang M, Guo Y, Hippe DS, Zhao X, Yuan C, Saba L, et al. Plaque RADS Related to Cerebrovascular Event Risk with Mild/moderate Stenosis: a CARE II study. AJNR Am J Neuroradiol 2025;46(11):2221–7. https://doi.org/10.3174/ajnr.A8819.

[72] Koo J. The Latest Information on Intracranial Atherosclerosis: Diagnosis and Treatment. Interv Neurol 2015;4:48–50. https://doi.org/10.1159/000438779.

[73] Chen LH, Spagnolo-Allende A, Yang D, Qiao Y, Gutierrez J. Epidemiology, Pathophysiology, and Imaging of Atherosclerotic Intracranial Disease. Stroke 2024;55:311–23. https://doi.org/10.1161/STROKEAHA.123.043630.

[74] Jeng J-S, Tang S-C, Liu H-M. Epidemiology, diagnosis and management of intracranial atherosclerotic disease. Expert Rev Cardiovasc Ther 2010;8:1423–32. https://doi.org/10.1586/erc.10.129.
[75] Sun J, Mossa-Basha M, Canton G, Balu N, Guo Y, Chen L, et al. Characterization of non-stenotic plaques in intracranial arteries with multi-contrast, multi-planar vessel wall image analysis. J Stroke Cerebrovasc Dis 2022;31:106719. https://doi.org/10.1016/j.jstrokecerebrovasdis.2022.106719.
[76] Bai X, Fan P, Li Z, Mossa-Basha M, Ju Y, Zhao X, et al. Evaluating Middle Cerebral Artery Plaque Characteristics and Lenticulostriate Artery Morphology Associated With Subcortical Infarctions at 7T MRI. J Magn Reson Imaging 2024;59:1045–55. https://doi.org/10.1002/jmri.28839.
[77] Nguyen-Huynh MN, Wintermark M, English J, Lam J, Vittinghoff E, Smith WS, et al. How accurate is CT angiography in evaluating intracranial atherosclerotic disease. Stroke 2008;39(4):1184–8. https://doi.org/10.1161/STROKEAHA.107.502906.
[78] Kim JM, Jung KH, Sohn CH, Moon J, Shin JH, Park J, et al. Intracranial plaque enhancement from high resolution vessel wall magnetic resonance imaging predicts stroke recurrence. Int J Stroke 2016;11(2):171–9. https://doi.org/10.1177/1747493015609775.
[79] Alexander MD, de Havenon A, Kim S-E, Parker DL, McNally JS. Assessment of quantitative methods for enhancement measurement on vessel wall magnetic resonance imaging evaluation of intracranial atherosclerosis. Neuroradiology 2019;61:643–50. https://doi.org/10.1007/s00234-019-02167-3.
[80] Gupta A, Baradaran H, Al-Dasuqi K, Knight-Greenfield A, Giambrone AE, Delgado D, et al. Gadolinium Enhancement in Intracranial Atherosclerotic Plaque and Ischemic Stroke: A Systematic Review and Meta-Analysis. JAHA 2016;5(8):e003816. 15.
[81] Lee HN, Ryu CW, Yun SJ. Vessel-Wall Magnetic Resonance Imaging of Intracranial Atherosclerotic Plaque and Ischemic Stroke: A Systematic Review and Meta-Analysis. Front Neurol 2018;3(9):1032. https://doi.org/10.3389/fneur.2018.01032.
[82] Song JW, Pavlou A, Xiao J, Kasner SE, Fan Z, Messé SR. Vessel Wall Magnetic Resonance Imaging Biomarkers of Symptomatic Intracranial Atherosclerosis: A Meta-Analysis. Stroke 2021;52:193–202. https://doi.org/10.1161/STROKEAHA.120.031480.
[83] Lee WJ, Choi HS, Jang J, Sung J, Kim TW, Koo J, et al. Non-stenotic intracranial arteries have atherosclerotic changes in acute ischemic stroke patients: a 3T MRI study. Neuroradiology 2015;57(10):1007–13. https://doi.org/10.1007/s00234-015-1566-9.
[84] Vergouwen MD, Silver FL, Mandell DM, Mikulis DJ, Swartz RH. Eccentric narrowing and enhancement of symptomatic middle cerebral artery stenoses in patients with recent ischemic stroke. Arch Neurol 2011;68(3):338–42. https://doi.org/10.1001/archneurol.2011.20. %252010.1001/archneurol.2011.20.
[85] Miura T, Matsukawa N, Sakurai K, Katano H, Ueki Y, Okita K, et al. Plaque vulnerability in internal carotid arteries with positive remodeling. Cerebrovasc Dis Extra 2011;1(1):54–65. https://doi.org/10.1159/000328645.
[86] Astor BC, Sharrett AR, Coresh J, Chambless LE, Wasserman BA. Remodeling of carotid arteries detected with MR imaging: atherosclerosis risk in communities carotid MRI study. Radiology 2010;256(3):879–86. https://doi.org/10.1148/radiol.10091162.
[87] Varnava AM, Mills PG, Davies MJ. Relationship between coronary artery remodeling and plaque vulnerability. Circulation 2002;105(8):939–43. https://doi.org/10.1161/hc0802.104327.
[88] Kharal GA, Ibrikji SE, Farag YM, Shoskes A, Kiczek MP, Sheth R, et al. Predictive Value of Clinical, CSF and Vessel Wall MRI Variables in Diagnosing Primary Angiitis of the CNS. Neurol Clin Pract 2024;14(4):e200321. https://doi.org/10.1212/CPJ.0000000000200321.
[89] Destrebecq V, Sadeghi N, Lubicz B, Jodaitis L, Ligot N, Naeije G. Intracranial Vessel Wall MRI in Cryptogenic Stroke and Intracranial Vasculitis. J Stroke Cerebrovasc Dis 2020;29(5):104684. https://doi.org/10.1016/j.jstrokecerebrovasdis.2020.104684.
[90] Diener HC, Easton JD, Hart RG, Kasner S, Kamel H, Ntaios G. Review and update of the concept of embolic stroke of undetermined source. Nat Rev Neurol 2022;18(8):455–65. https://doi.org/10.1038/s41582-022-00663-4.
[91] Hart RG, Catanese L, Perera KS, Ntaios G, Connolly SJ. Embolic Stroke of Undetermined Source: A Systematic Review and Clinical Update. Stroke 2017;48:867–72. https://doi.org/10.1161/STROKEAHA.116.016414.
[92] Saver JL. Cryptogenic Stroke. 15 N Engl J Med 2016;375(11):e26. https://doi.org/10.1056/NEJMc1609156.
[93] Schaafsma JD, Rawal S, Coutinho JM, Rasheedi J, Mikulis DJ, Jaigobin C, et al. Diagnostic Impact of Intracranial Vessel Wall MRI in 205 Patients with Ischemic Stroke or TIA. AJNR Am J Neuroradiol 2019;40:1701–6. https://doi.org/10.3174/ajnr.A6202.
[94] Das S, Mossa-Basha M, Dey M, Hazra A, Pandit A, Das G, et al. High-resolution vessel wall magnetic resonance imaging in intracranial vasculopathies: an experience from eastern India. Br J Radiol 2023;96(1145):20230114. https://doi.org/10.1259/bjr.20230114.
[95] Adams HP, Bendixen BH, Kappelle LJ, Biller J, Love BB, Gordon DL, et al. Classification of subtype of acute ischemic stroke. Definitions for use in a multicenter clinical trial. TOAST. Trial of Org 10172 in Acute Stroke Treatment. Stroke 1993;24:35–41. https://doi.org/10.1161/01.str.24.1.35.
[96] Kesav P, Krishnavadana B, Kesavadas C, Sreedharan SE, Rajendran A, Sukumaran S, et al. Utility of intracranial high-resolution vessel wall magnetic resonance imaging in differentiating intracranial vasculopathic diseases causing ischemic stroke. Neuroradiology 2019;61(4):389–96. https://doi.org/10.1007/s00234-019-02157-5.
[97] Tandon V, Senthilvelan S, Sreedharan SE, Kesavadas C, Vt J, Sylaja PN. High-resolution MR vessel wall imaging in determining the stroke aetiology and risk stratification in isolated middle cerebral artery disease. Neuroradiology 2022;64(8):1569–77. https://doi.org/10.1007/s00234-021-02891-9.
[98] He WW, Lu SS, Ge S, Gu P, Shen ZZ, Wu FY, et al. Impact on etiology diagnosis by high-resolution vessel wall imaging in young adults with ischemic stroke or transient ischemic attack. Neuroradiology 2023;65:1015–23. https://doi.org/10.1007/s00234-023-03131-y.
[99] Yoon Y, Lee DH, Kang DW, Kwon SU, Kim JS. Single subcortical infarction and atherosclerotic plaques in the middle cerebral artery: high-resolution magnetic resonance imaging findings. Stroke 2013;44(9):2462–7. https://doi.org/10.1161/STROKEAHA.113.001467.
[100] Klein IF, Lavallée PC, Mazighi M, Schouman-Claeys E, Labreuche J, Amarenco P. Basilar artery atherosclerotic plaques in paramedian and lacunar pontine infarctions: a high-resolution MRI study. Stroke 2010;41(7):1405–9. https://doi.org/10.1161/STROKEAHA.110.583534.
[101] Marquering HA, Nederkoorn PJ, Beenen LF, Lycklama à Nijeholt GJ, van den Berg R, Roos YB, et al. Carotid pseudo-occlusion on CTA in patients with acute ischemic stroke: a concerning observation. Clin Neurol Neurosurg 2013;115:1591–4. https://doi.org/10.1016/j.clineuro.2013.02.008.
[102] Chai S, Sheng Z, Xie W, Wang C, Liu S, Tang R, et al. Assessment of Apparent Internal Carotid Tandem Occlusion on High-Resolution Vessel Wall Imaging: Comparison with Digital Subtraction Angiography. AJNR Am J Neuroradiol 2020;41:693–9. https://doi.org/10.3174/ajnr.A6452.
[103] Zhang X, Zhou C, Cao Y-Z, Su C-Q, Shi H-B, Lu S-S, et al. High-resolution magnetic resonance imaging for predicting successful recanalization in patients with chronic internal carotid artery occlusion. Front Neurol 2022;13:1003800. https://doi.org/10.3389/fneur.2022.1003800.
[104] Zhang J, Ding S, Zhao H, Sun B, Li X, Zhou Y, et al. Evaluation of chronic carotid artery occlusion by non-contrast 3D-MERGE MR vessel wall imaging: comparison with 3D-TOF-MRA, contrast-enhanced MRA, and DSA. Eur Radiol 2020;30:5805–14. https://doi.org/10.1007/s00330-020-06989-1.
[105] Zhang J, Ding S, Zhao B, Sun B, Guo Q, Pan Y, et al. Morphological and Compositional Features of Chronic Internal Carotid Artery Occlusion in MR Vessel Wall Imaging Predict Successful Endovascular Recanalization. Diagnostics (Basel) 2023;13(147). https://doi.org/10.3390/diagnostics13010147.
[106] Wan M, Yan L, Xu Z, Hou Z, Kang K, Cui R, et al. Symptomatic and Asymptomatic Chronic Carotid Artery Occlusion on High-Resolution MR Vessel Wall Imaging. AJNR Am J Neuroradiol 2022;43:110–6. https://doi.org/10.3174/ajnr.A7365.
[107] Sajedi PI, Gonzalez JN, Cronin CA, Kouo T, Steven A, Zhuo J, et al. Carotid Bulb Webs as a Cause of “Cryptogenic” Ischemic Stroke. AJNR Am J Neuroradiol 2017;38:1399–404. https://doi.org/10.3174/ajnr.A5208.
[108] Wojcik K, Milburn J, Vidal G, Tarsia J, Steven A. Survey of Current Management Practices for Carotid Webs. Ochsner J 2019;19:296–302. https://doi.org/10.31486/toj.18.0114.
[109] Gopal N, Gupta V, Bhatt AA, Middlebrooks EH. Teaching NeuroImages: Vessel wall imaging of carotid web. Neurology 2020;95:e2174–5. https://doi.org/10.1212/WNL.0000000000010350.
[110] Boesen ME, Eswaradass PV, Singh D, Mitha AP, Goyal M, Frayne R, et al. MR imaging of carotid webs. Neuroradiology 2017;59:361–5. https://doi.org/10.1007/s00234-017-1797-z.
[111] Talathi S, Lipsitz EC. Current Therapy for Carotid Webs. Ann Vasc Surg 2025;113:415–20. https://doi.org/10.1016/j.avsg.2024.08.014.
[112] Rutman AM, Vranic JE, Mossa-Basha M. Imaging and Management of Blunt Cerebrovascular Injury. Radiographics 2018;38:542–63. https://doi.org/10.1148/rg.2018170140.
[113] Pfefferkorn T, Saam T, Rominger A, Habs M, Gerdes L-A, Schmidt C, et al. Vessel wall inflammation in spontaneous cervical artery dissection: a prospective, observational positron emission tomography, computed tomography, and magnetic resonance imaging study. Stroke 2011;42:1563–8. https://doi.org/10.1161/STROKEAHA.110.599548.
[114] Habs M, Pfefferkorn T, Cyran CC, Grimm J, Rominger A, Hacker M, et al. Age determination of vessel wall hematoma in spontaneous cervical artery dissection: a multi-sequence 3T cardiovascular magnetic resonance study. J Cardiovasc Magn Reson 2011;13:76. https://doi.org/10.1186/1532-429X-13-76.
[115] Arning C, Hanke-Arning K, Eckert B. The Clinical Features of Dissection of the Cervical Brain-Supplying Arteries. Dtsch Arztebl Int 2022;119:581–7. https://doi.org/10.3238/arztebl.m2022.0238.
[116] Huang RJ, Lu Y, Zhu M, Zhu JF, Li YG. Simultaneous non-contrast angiography and intraplaque haemorrhage (SNAP) imaging for cervical artery dissections. e7 Clin Radiol 2019;74(817):e1–817. https://doi.org/10.1016/j.crad.2019.06.018.
[117] Xia S, Wang Y, Lv X, Chen C, Hui J, Wu X, et al. The use of SNAP and T1-weighted VISTA in cervical artery dissection. Interv Neuroradiol 2023;29:235–42. https://doi.org/10.1177/15910199221082847.
[118] Wu Y, Wu F, Liu Y, Fan Z, Fisher M, Li D, et al. High-Resolution Magnetic Resonance Imaging of Cervicocranial Artery Dissection: Imaging Features Associated With Stroke. Stroke 2019;50:3101–7. https://doi.org/10.1161/STROKEAHA.119.026362.
[119] Bonow RH, Witt CE, Mosher BP, Mossa-Basha M, Vavilala MS, Rivara FP, et al. Transcranial Doppler Microemboli Monitoring for Stroke Risk Stratification in Blunt Cerebrovascular Injury. Crit Care Med 2017;45:e1011–7. https://doi.org/10.1097/CCM.0000000000002549.
[120] Wu L, Christensen D, Call L, Vranic J, Colip C, Hippe DS, et al. Natural History of Blunt Cerebrovascular Injury: Experience Over a 10-year Period at a Level I Trauma Center. Radiology 2020;297:428–35. https://doi.org/10.1148/radiol.2020192866.

[121] Bonow RH, Witt CE, Mossa-Basha M, Cuschieri J, Arbabi S, Vavilala MS, et al. Aspirin versus anticoagulation for stroke prophylaxis in blunt cerebrovascular injury: a propensity-matched retrospective cohort study. J Neurosurg 2021;135:1413–20. https://doi.org/10.3171/2020.10.JNS201836.
[122] Vranic JE, Huynh TJ, Fata P, Barber J, Bonow RH, Levitt MR, et al. The ability of magnetic resonance black blood vessel wall imaging to evaluate blunt cerebrovascular injury following acute trauma. J Neuroradiol 2020;47:210–5. https://doi.org/10.1016/j.neurad.2019.01.091.
[123] Wang M, Yang Y, Zhou F, Li M, Liu R, Guan M, et al. The Contrast Enhancement of Intracranial Arterial Wall on High-resolution MRI and Its Clinical Relevance in Patients with Moyamoya Vasculopathy. Sci Rep 2017;7:44264. https://doi.org/10.1038/srep44264.
[124] Ryoo S, Cha J, Kim SJ, Choi JW, Ki CS, Kim KH, et al. High-resolution magnetic resonance wall imaging findings of Moyamoya disease. Stroke 2014;45(8):2457–60. https://doi.org/10.1161/STROKEAHA.114.004761.
[125] Digpal R, Arkill KP, Doherty R, Yates J, Milne LK, Broomes N, et al. A Systematic Review and Meta-Analysis of the Pathology Underlying Aneurysm Enhancement on Vessel Wall Imaging. IJMS 2024;25:2700. https://doi.org/10.3390/ijms25052700.
[126] Texakalidis P, Hilditch CA, Lehman V, Lanzino G, Pereira VM, Brinjikji W. Vessel Wall Imaging of Intracranial Aneurysms: Systematic Review and Meta-analysis. World Neurosurgery 2018;117(453-458):e1. https://doi.org/10.1016/j.wneu.2018.06.008.
[127] Samaniego EA, Roa JA, Hasan D. Vessel wall imaging in intracranial aneurysms. J NeuroIntervent Surg 2019;11:1105–12. https://doi.org/10.1136/neurintsurg-2019-014938.
[128] Hsu CC-T, Suthiphosuwan S, Huynh T, Murphy A, Li Y, Bharatha A, High-Resolution MRI. Vessel Wall Imaging in Acute Aneurysmal Subarachnoid Hemorrhage: Spatiotemporal Pattern and Clinicoradiologic Implications. Clin Neuroradiol 2020;30:801–10. https://doi.org/10.1007/s00062-019-00843-8.
[129] Guo Y, Canton G, Chen L, Sun J, Geleri DB, Balu N, et al. Multi-Planar, Multi-Contrast and Multi-Time Point Analysis Tool (MOCHA) for Intracranial Vessel Wall Characterization. Magnetic Resonance Imaging 2022;56(3):944–55. https://doi.org/10.1002/jmri.28087.
[130] Chen L, Zhao H, Jiang H, Balu N, Geleri DB, Chu B, et al. Domain adaptive and fully automated carotid artery atherosclerotic lesion detection using an artificial intelligence approach (LATTE) on 3D MRI. Magn Reson Med 2021;86:1662–73. https://doi.org/10.1002/mrm.28794.
[131] Song JW, Phi HQ, Koneru M, Cao Q, Rubin J, Sakai Y, et al. Prevalence of High-Risk CTA-Based Carotid Plaque-RADS Subtypes in Patients With Embolic Stroke of Undetermined Source. Stroke 2025;56:737–40. https://doi.org/10.1161/STROKEAHA.124.048305.
[132] Saba L, Mannelli L, Balestrieri A, Serra A, Bassareo P, Murgia A, et al. CT and MR Imaging of Carotid Wall and Plaque. J Neurosonol Neuroimag 2019;11:115–25. https://doi.org/10.31728/jnn.2019.00062.
[133] Baradaran H, Gupta A. Carotid Vessel Wall Imaging on CTA. AJNR Am J Neuroradiol 2020;41:380–6. https://doi.org/10.3174/ajnr.A6403.
[134] Nielsen RV, Fuster V, Bundgaard H, Fuster JJ, Johri AM, Kofoed KF, et al. Personalized Intervention Based on Early Detection of Atherosclerosis. Journal of the American College of Cardiology 2024;83:2112–27. https://doi.org/10.1016/j.jacc.2024.02.053.